

Thesis on

Design of a Control Algorithm for Recoil Mitigation of a Multi rotor Unmanned Combat Aerial Vehicle

Submitted in fulfillment of the requirements

for the degree of

Master of Technology

by

Ishwar Hebbar (163109005)

under the guidance of

Prof. Abhishek Gupta



Department of Mechanical Engineering

Indian Institute of Technology, Bombay

Certificate

This is to certify that the thesis titled "**Design of a Control Algorithm for Recoil Mitigation of a Multi rotor Unmanned Combat Aerial Vehicle**" by **Ishwar Hebbar (163109005)**, has been carried out under my supervision in fulfilment of the requirement for the degree of **Master of Technology** during the session 2018-19 in the Department of Mechanical Engineering, Indian Institute of Technology, Bombay.

Prof. Abhishek Gupta
(Project Guide)
Department of Mechanical Engineering
IIT Bombay

Declaration

I hereby declare that, the report has been written by me in my own words and source(s) of material used in the report have been duly acknowledged as and where applicable. I understand that, copying material from a published book, journal, dissertation/thesis, authored report, website etc. without a proper acknowledgement and presenting as work done by me is a serious offence. The contents presented in this report are original research contribution and the same are not submitted to any other institute or university for award of any degree or diploma.

Ishwar Hebbar (163109005)

Department of Mechanical Engineering
IIT Bombay

Acknowledgement

I wish to express my heartfelt thanks and deep sense of gratitude to Prof. Abhishek Gupta for his excellent guidance and whole hearted involvement during the course of this work. I am also indebted to him for his encouragement and moral support throughout the project. I am also thankful to him for the valuable time that he has provided with the practical guidance at every step of the project work. The help, support and encouragement offered by Mr. Mahesh Kotnis, Mr. Gauresh Shirodkar and Mr. Indrajeet Desai in research work is gratefully acknowledged. I would like to express my gratitude towards my family for their kind co-operation and encouragement which helped me in this project.

Ishwar Hebbar (163109005)

Department of Mechanical Engineering

IIT Bombay

Contents

Abstract	a
1 Introduction	1
2 Literature Review	4
2.1 Introduction	4
2.2 Modelling	6
2.2.1 Newtonian Equations of Motion	6
2.2.2 Eulerian Equations of Motion	8
2.3 Quadcopter Dynamics	10
2.3.1 Kinematics	10
2.3.2 Motor Modelling	11
2.3.3 Forces	12
2.3.4 Torques	13
2.3.5 Equations of Motion	14
2.4 Quadcopter Simulation	18
2.5 Quadcopter Control	19
2.6 Recoil Modelling	24
3 Effect of Control Gains on Stability of a PLD mounted Quadcopter	27
3.1 Models Considered	27
3.1.1 6 DOF Planar System	27
3.1.2 Three DOF Model	32

3.2	Methodology for tuning controller gains using spring mass Damper analogy	36
4	Experimental Setup	41
4.1	SolidWorks Model of the Setup	42
4.2	Gun Selection	44
4.2.1	Gun Actuation Mechanisms	45
4.3	Quadcopter Size Selection	46
4.4	Mathematical Model and Simulation in MATLAB of the Experimental Setup	48
4.5	Full Setup	51
4.6	Mathematical Model Validation with actual setup	53
4.7	Simulation to Obtain Control Gains	54
4.8	Sensors	55
5	Experiments	60
5.1	Benchmarking of Gun Aim and Precision	60
5.1.1	Benchmarking of the Gun Aim and Precision on Setup	62
5.1.2	Effect of control Algorithms on Precision, Accuracy and Firing Rates	64
5.2	Results and Discussion	65
6	Conclusions	67
References		69

List of Figures

1.1	Oehmichen No.2 Quadrotor [1]	1
1.2	U.S. Air Force photo by Paul Ridgeway [2]	2
1.3	an image of a Taiwanese company's Machine Gun Mounted UCAV[3]	2
2.1	Tait – Bryan angle rotations in Z X Y order [4]	6
2.2	Roll Pitch and Yaw angles [4]	7
2.3	Quadcopter Body Frame and Inertial Frame [5]	10
2.4	Simulation of Quadcopter motion	18
2.5	Angular Deflection vs. Time I& Angular Velocity vs. time –MATLAB simulation	22
2.6	Angular Deflection vs. Time I& Angular Velocity vs. time –Reference Paper [5]	23
2.7	Ashani Mark – II Pistol – Made in India [6]	24
2.8	Pressure vs Time of ASHANI MARK -II Pistol [6]	26
3.1	Six DOF planar Model	27
3.2	UCAV by Duke Robotics [3]	27
3.3	Free body diagram of the Quadcoptor	28
3.4	Free Body Diagram of the PLD	29
3.5	Simulation of the Six DOF model - 1	30
3.6	Simulation of the Six DOF model - 2	30
3.7	Variation of the PLD states namely x_2, y_2 and ϕ with time	31
3.8	Three DOF MATLAB model	32

3.9	A DIY Gun monted Quadcoptor [7]	32
3.10	Three DOF MATLAB model	33
3.11	Simulation of Three DOF Model	33
3.12	Simulation Results of the Three DOF model	34
3.13	Impulse Response of the Three DOF model	35
3.14	6_{th} order Transfer function of the linearized three DOF mode	36
3.15	Crests and troughs of the Impulse response of the Three DOF Model	37
3.16	Variation of Zeta with Proportional Gain and Derivative Gain	38
3.17	Variation of Damped oscillation frequency ω_d with Proportional Gain and Derivative Gain	39
4.1	Long Cantilever Type	42
4.2	Paeucelliers Mechanism Type	42
4.3	Cross Section of Cantilever	43
4.4	Cantilever Beam	43
4.5	Toy Gun	44
4.6	Toy Shotgun	44
4.7	Air Gun	45
4.8	Linear Actuator	45
4.9	Linear Actuator Coupled With Trigger	45
4.10	Motor with Steel String attached to The Trigger - 1	46
4.11	Motor with Steel String attached to The Trigger - 2	46
4.12	2D Quadcoptor	47
4.13	EOM with out Gun	48
4.14	EOM with Gun	49
4.15	Full Setup 1	51
4.16	Full Setup 2	51
4.17	Angular Displacement (Theta) Vs. Time of the Mathematical Model	53
4.18	Linear Displacement (X) Vs. Time of the Mathematical Model	53

4.19	Angular Displacement (Theta) Vs. Time of the Mathematical Model(blue) and IMU values from the setup(red)	53
4.20	Linear Displacement (X) Vs. Time of the Mathematical Model(blue) and IMU values from the setup(red)	53
4.21	Ashani Mark – II Pistol – Made in India [19] [6]	54
4.22	Recoil force used in Simulation to approximate the actual gun recoil	54
4.23	Simulated output of Theta Vs. time for a PD Controller	55
4.24	Simulated output of X Vs. time for a PD Controller	55
4.25	Strain Gauge on Cantilever beam	56
4.26	vishay strain gauge indicator model P3	57
4.27	Inertial Measurement Unit MPU6050	58
5.1	Benchmarking affixed to the ground 1	60
5.2	Benchmarking affixed to the ground 2	60
5.3	Progressive Shot Patterns	62
5.4	Scatter pattern of gun mounted on setup	63
5.5	Experiments with different controllers)	65
5.6	Experiments with different controllers	66

Abstract

The drone industry has taken leaps and bounds in the last five years. Drones are used in a myriad range of applications from deliveries (Amazon, Flipkart, etc.), surveillance, bomb disposal, toys, weapons, and even to shoot movies and videos. There is a subtype of drones which have a projectile launching device on it, for example, guns, water cannons, etc.

There are a variety of applications involving drones launching projectiles, ranging from military applications to surveillance bug planting. In the case a projectile is launched from a drone, the standard control algorithms are insufficient to optimally control the drone to maximize the accuracy of the projectile. This report focuses on a methodology to design such a control system through the use of analogous spring-damper systems, in particular for a Quadcopter.

An ASHANI MARK -II Pistol was selected as the PLD and its Average Recoil Force, Barrel time, etc. were calculated. For simplicity, a planar model of a Quadcopter was considered. In the first model, the PLD and the Quadcopter were allowed 3 DOF's each resulting in a 6 DOF model. The behaviour of this model was noted for some values of gains as well as spring-damper coefficients. In the next model, the PLD was rigidly attached to the Quadcopter resulting in a 3 DOF model. In this model, the impulse response to each input, i.e., X impulse, Y impulse, and θ impulse to each output, X – displacement, Y – displacement and θ – displacement was plotted.

A second order Transfer Function was fitted onto the impulse responses, and an analogous spring damper system was formulated. The response of the formulated system was plotted, and the analogous nature was verified.

The values of the spring stiffness and the damping coefficient in the analogous system were tuned using the empirical relationship between the gains and the coefficients.

A setup was built in order to test the control system and fine tune the control gains.

Several control strategies like PD, PID and PID on both x and θ states were used and their effects on the accuracy, precision and firing rates were studied.

Chapter 1

Introduction

History of Quadcopter

The idea for a multi-rotor flying machine isn't new; in fact, the first recorded flight of a Quadcopter system was in 1907, a four-rotor helicopter designed by Louis Breguet. This system was the first rotary wing aircraft to lift itself off the ground, although only in tethered flight at an altitude of a few feet. In 1908 it was reported as having flown 'several times,' although details are sparse [8].

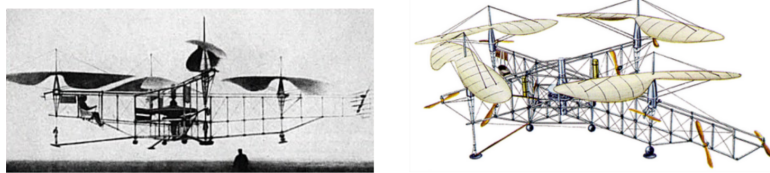


Figure 1.1: Oehmichen No.2 Quadrotor [1]

The helicopter was the most proliferated 2 bladed system used until very recently due to its ease of control in comparison to the Quadcopter system. A conventional helicopter usually has two coplanar rotors having the thrust vector pointing upwards, the balance of a conventional helicopter was done using a gyroscopic mechanism which made the system inherently stable.

Unmanned Combat Ariel Vehicles (UCAV's)

An unmanned combat aerial vehicle (UCAV), also known as a combat drone or simply a drone, is an unmanned aerial vehicle (UAV) that usually carries aircraft ordnance such as missiles and is used for drone strikes [9] [10]. Aircraft of this type have no onboard human pilot [11]. These drones are usually under real-time human control, with varying levels of autonomy [12].



Figure 1.2: U.S. Air Force photo by Paul Ridgeway [2]



Figure 1.3: an image of a Taiwanese company's Machine Gun Mounted UCAV[3]

Equipment necessary for a human pilot (such as the cockpit, armor, ejection seat, flight controls, and environmental controls for pressure and oxygen) are not needed, as the operator runs the vehicle from a remote terminal, resulting in a lower weight and a smaller size than a manned aircraft.

Motivation and Objective

The Unmanned Combat Ariel Vehicle (UCAV) is gaining more and more popularity in the drone industry, both for military purposes and for drone based games. This type of drone will be useful in a variety of applications from shooting zip lines to planting trackers/cameras onto specific surfaces for video/audio surveillance.

The accuracy of such projectile shooting devices currently depends highly on the experience of the operator, and thus, widespread utility is not in place currently. It is necessary to design such a controller so as to maximize the accuracy of a projectile shooting device and make it less dependent on operator skills.

Chapter 2

Literature Review

2.1 Introduction

The technology mounting PLD's on autonomous Quadcoptor drones is a new and unexplored area with several ethical and technical difficulties, as such not many publications can be found on this sensitive topic. On the other hand DIY video maker all around the world including several military contractors in the US have already created such PLD mounted Quadcopters [3]. As such the only information we have comes from their websites and the videos documenting the behavior of such Quadcopters.

From the company's promotional video [3], it is clearly stated that the major technology involved in the mounting of the PLD on the Quadcoptor is the novel Gimbal arrangement they have put forth. This according to the video reduced the major issue of PLD mounted UCAV's which is the dissipation of recoil force. The two issues they deal with are the accuracy degradation due to the nature of the Quadcoptor and the delay in firing the second round due to the time required by the Quadcoptor to stabilize after firing the first round. Therefore we must first study recoil.

The recoil due to launching a projectile is generally dissipated in two stages, the first stage is the buffering mechanism in the launcher itself and the second stage is by the ground support of the launcher.

In order to bring the rearward moving gun to a halt, the momentum acquired by the

gun is dissipated by a forward acting counter-recoil force applied to the gun over a period of time after the projectile exits the muzzle. To apply this counter-recoiling force, modern mounted guns may employ recoil buffering comprising springs and hydraulic recoil mechanisms, similar to shock absorbing suspension on automobiles. Early cannons used systems of ropes along with rolling or sliding friction to provide forces to slow the recoiling cannon to a stop. Recoil buffering allows the maximum counter-recoil force to be lowered so that strength limitations of the gun mount are not exceeded. Gun chamber pressures and projectile acceleration forces are tremendous, on the order of tens of thousands of pounds per square inch and tens of thousands of times the acceleration of gravity (g's), both necessary to launch the projectile at useful velocity during the very short travel distance of the barrel. However, the same pressures acting on the base of the projectile are acting on the rear face of the gun chamber, accelerating the gun rearward during firing. Practical weight gun mounts are typically not strong enough to withstand the maximum forces accelerating the projectile during the short time the projectile is in the barrel, typically only a few milliseconds. To mitigate these large recoil forces, recoil buffering mechanisms spread out the counter-recoiling force over a longer time, typically ten to a hundred times longer than the duration of the forces accelerating the projectile. This results in the required counter-recoiling force being proportionally lower, and easily absorbed by the gun mount. Modern cannons also employ muzzle brakes very effectively to redirect some of the propellant gasses rearward after projectile exit. This provides a counter-recoiling force to the barrel, allowing the buffering system and gun mount to be more efficiently designed at even lower weight. "Recoilless" guns, (recoilless rifle), also exist where much of the high pressure gas remaining in the barrel after projectile exit is vented rearward through a nozzle at the back of the chamber, creating a large counter-recoiling force sufficient to eliminate the need for heavy recoil mitigating buffers on the mount.

2.2 Modelling

The first step in any robotics related application is to derive the Equations of motion of the system of concern. This can be done in several approaches as explained below

2.2.1 Newtonian Equations of Motion

The first generalized equations of motion were derived from Newton's Second Law, which states that, Change in momentum is equal to external force. In order to use these equations in Drone Applications to find acceleration both linear and angular we need to introduce the concept of Euler angles. The Euler angles are three angles introduced by Leonhard Euler to describe the orientation of a rigid body with respect to a fixed coordinate system [13]. They can also represent the orientation of a mobile frame of reference in physics or the orientation of a general basis in 3-dimensional linear algebra. There are two sets of these angles namely the Proper Euler angles and Tait–Bryan angles. These are differentiated according to whether the consecutive rotations are done around the inertial/Fixed Frame of reference (Tait–Bryan) or whether they are done around the rotating frame of reference itself (Proper Euler).

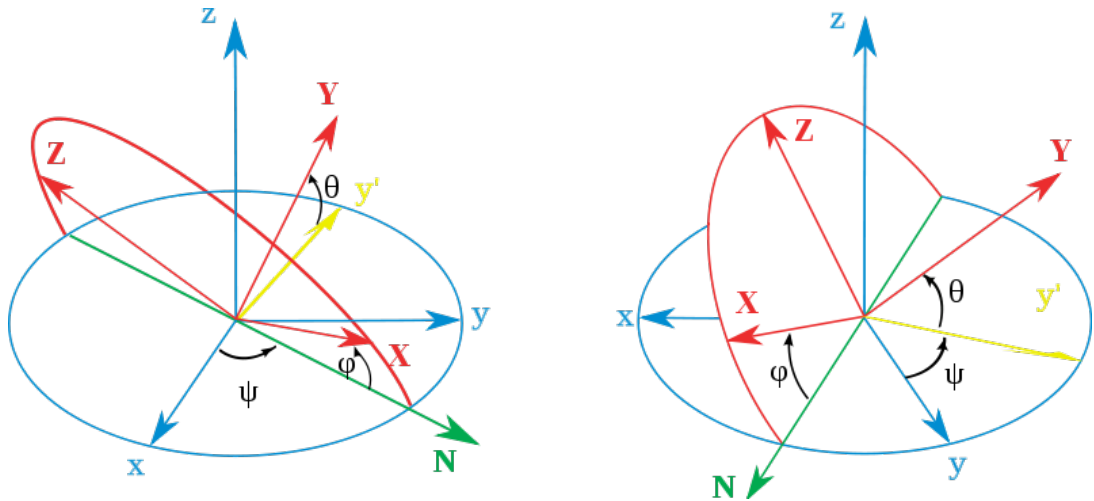


Figure 2.1: Tait – Bryan angle rotations in Z X Y order [4]

The more popular of the two in the drone industry are the Tait-Bryan angles, they are also known as the Roll, Pitch and Yaw angles. Even in the Tait-Bryan angles there is ambiguity on the order of rotations to reach the final frame so there are 6 Rotation Matrices corresponding to the different orders of the rotations. For Ex, Tait Bryan Rotation matrix corresponding to $Z_1X_2Y_3$ order is

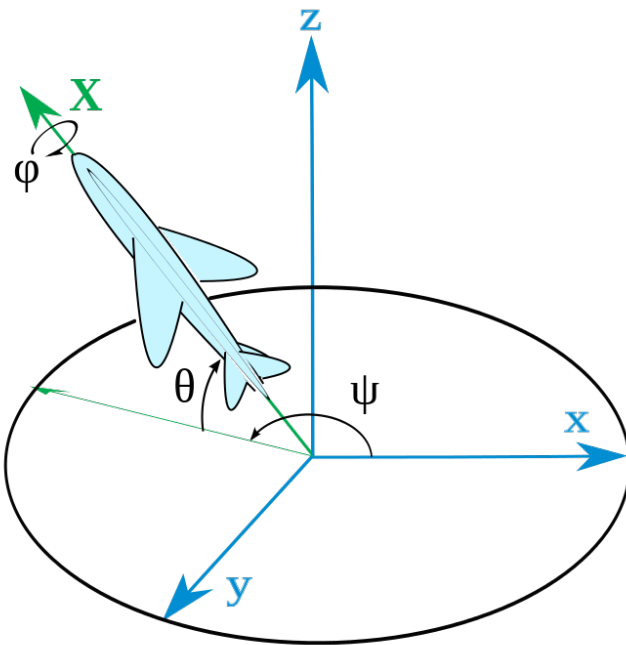


Figure 2.2: Roll Pitch and Yaw angles [4]

$${}^I_B R = \begin{bmatrix} c\theta c\psi & s\theta s\phi c\psi - s\psi c\phi & s\theta c\phi c\psi + s\psi s\phi \\ c\theta s\psi & s\theta s\phi s\psi + c\psi c\phi & s\theta c\phi s\psi - c\psi s\phi \\ -s\theta & c\theta s\phi & c\theta c\phi \end{bmatrix} \quad (2.1)$$

Where

θ is the angle of roll

ϕ is the angle of pitch

ψ is the angle of yaw

Where ${}^I_B R$ is the rotation matrix that takes a vector from the body frame of reference to the inertial frame of reference. This gives us the way to transform forces from a body frame of reference and back.

The time derivative of Euler angles are not equal to the angular velocities in Body frame of reference, and so to find the relationship between them we use the inverted Wronskian Matrix denoted by [5]

$$W^{-1} = \frac{1}{c\theta} \begin{bmatrix} c\theta & s\phi s\psi & c\phi s\theta \\ 0 & c\phi c\theta & -s\phi c\theta \\ 0 & s\phi & c\phi \end{bmatrix} \quad (2.2)$$

Which gives us the relation between the time derivative of Euler angles and angular velocities in the body frame of reference.

$$\frac{d}{dt} \text{EulerAngles} = W^{-1} \omega_b \quad (2.3)$$

With this Knowledge now it is possible to write the Equations of motion for a general drone

$${}^I_B R F_B = m a_1 \quad (2.4)$$

$${}^I_B R \tau_B = \frac{d I_1}{dt} {}^I_B R \omega_B + \frac{d({}^I_B R \omega_B)}{dt} I_1 \quad (2.5)$$

In this case the computations become cumbersome and hardly anyone uses these equations in rigid body dynamics these days.

2.2.2 Eulerian Equations of Motion

In classical mechanics, Euler's rotation equations are a vectorial quasi linear first-order ordinary differential equation describing the rotation of a rigid body, using a rotating reference frame with its axes fixed to the body and parallel to the body's principal axes of inertia. Their general form is: [14]

$$I\dot{\omega} + \omega \times (I\omega) = M \quad (2.6)$$

Where M is the applied torques, I is the inertia matrix, and ω is the angular velocity about the principal axes.

In 3D principal orthogonal coordinates, they become:

$$I_1\dot{\omega}_1 + (I_3 - I_2)\omega_2\omega_3 = M_1 \quad (2.7)$$

$$I_2\dot{\omega}_2 + (I_1 - I_3)\omega_3\omega_1 = M_2 \quad (2.8)$$

$$I_3\dot{\omega}_3 + (I_2 - I_1)\omega_1\omega_2 = M_3 \quad (2.9)$$

Where M_k are the components of the applied torques are, I_k are the principal moments of inertia and ω_k are the components of the angular velocity about the principal axes. [11]

2.3 Quadcopter Dynamics

For dynamics first we have to create the proper frames of reference so the following are the two frames of reference we will be using. [5]

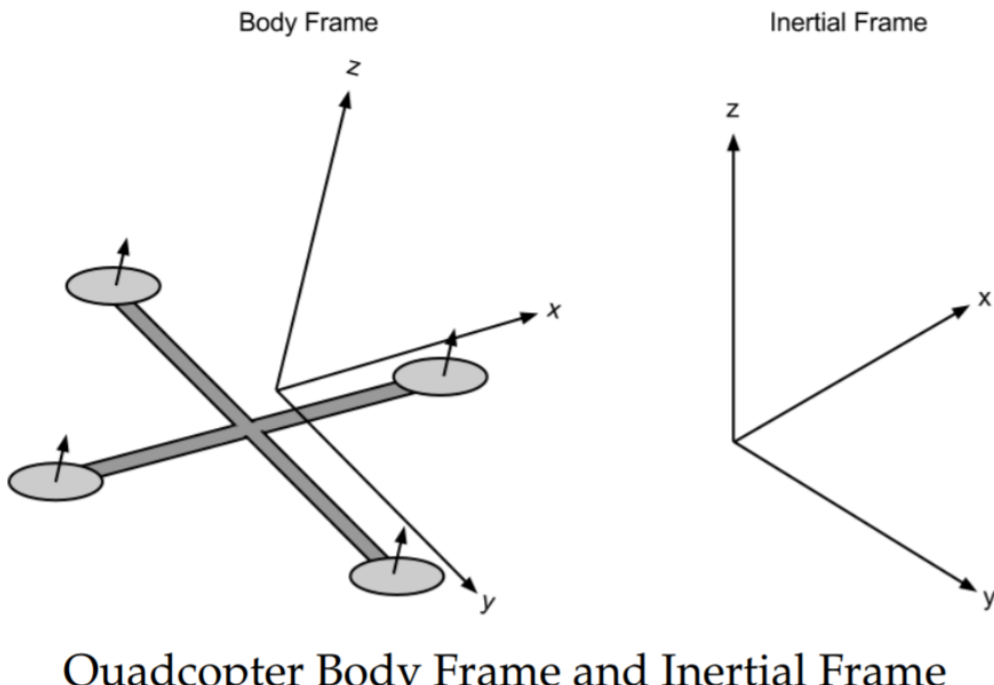


Figure 2.3: Quadcopter Body Frame and Inertial Frame [5]

2.3.1 Kinematics

Before going to the dynamics the kinematic relations need to be established clearly. The states that we will be using are Linear Displacement in space w.r.t. inertial frame ($(x = (x_i, y_i, z_i))$), Angular Displacement in Space w.r.t inertial frame ($\theta = (\phi, \theta, \psi)$), Linear Velocity in space w.r.t. inertial frame ($\dot{x} = (\dot{x}_i, \dot{y}_i, \dot{z}_i)$) and Angular Velocity in Space w.r.t Body frame ($\omega = (\dot{p}_b, \dot{q}_b, \dot{r}_b)$).

In addition to these we will also require the time derivatives of the angular displacements ($\dot{\theta} = (\dot{\phi}, \dot{\theta}, \dot{\psi})$)

So the Kinematic Equations relating these variables are

$$\dot{\theta} = W^{-1}\omega \quad (2.10)$$

where

$$W^{-1} = \frac{1}{c\theta} \begin{bmatrix} c\theta & s\phi s\psi & c\phi s\theta \\ 0 & c\phi c\theta & -s\phi c\theta \\ 0 & s\phi & c\phi \end{bmatrix} \quad (2.11)$$

And we will be using $Z_1 Y_2 X_3$ Tait Bryan Angles so the relation is

$$[\text{inertial frame vector}]_{3 \times 1} =_B^I R [\text{Body frame vector}]_{3 \times 1} \quad (2.12)$$

2.3.2 Motor Modelling

All Quadcoptor use Brush less DC motors and thus modelling one should be enough to cover all the actuators on a Quadcoptor. Now for an Electric motor we have the following equations

$$\tau = k_t(I - I_0) \quad (2.13)$$

$$V = IR_m + k_v\omega \quad (2.14)$$

τ - Torque Applied by the Motor

k_t - Torque proportionality constant

I_0 - No load Current

R_m - Motor Resistance

k_v - Proportionality constant relating Back EMF to RPM

ω - Angular velocity of motor shaft

For simplicity of modelling we assume small I_0 and R_m leaving us with the power equation as follows

$$p = VI \approx \frac{k_v}{k_t} \tau \omega \quad (2.15)$$

p is the power input to the system

2.3.3 Forces

The power spent by the Quadcopter is equal to the force generated on the propeller times the distance moved by the air. Assuming surrounding air velocity as zero, this gives us the equation

$$pdt = Tdx \quad (2.16)$$

$$pdt = T \frac{dt}{dx} \quad (2.17)$$

$$pdt = T v_h \quad (2.18)$$

v_h is the hover velocity

Momentum theory gives us an equation for hover velocity as a function of thrust

$$v_h = \sqrt{\frac{T}{2\rho A}} \quad (2.19)$$

Where ρ is the air density and A is the area swept by the rotor

We also know that,

$$\tau = k_\tau T \quad (2.20)$$

Where k_τ is the constant of proportionality relating torque to thrust

From the previous equations now we get

$$\frac{k_v k_\tau}{k_t} T \omega = \frac{T^{\frac{3}{2}}}{\sqrt{2\rho A}} \quad (2.21)$$

Solving for the thrust magnitude T , we obtain that thrust is proportional to the square of angular velocity of the motor

$$T = \left(\frac{k_v k_t \sqrt{2\rho A}}{k_\tau} \omega \right)^2 = k \omega^2 \quad (2.22)$$

Where k is some appropriately dimensioned constant

Now the forces on the Quadcopter in the Body frame are

$$ThrustForce = T_b = k \begin{bmatrix} 0 \\ 0 \\ \omega_1^2 - \omega_2^2 + \omega_3^2 - \omega_4^2 \end{bmatrix} \quad (2.23)$$

Where the subscripts stand for the i^{th} motor

$$DragForceF_D = \begin{bmatrix} -k_d \dot{x}_i \\ -k_d \dot{y}_i \\ -k_d \dot{z}_i \end{bmatrix} \quad (2.24)$$

2.3.4 Torques

Each rotor contributes some torque about the body z axis. This torque is the torque required to keep the propeller spinning and providing thrust; it creates the instantaneous angular acceleration and overcomes the frictional drag forces. The drag equation from fluid dynamics gives us the frictional force: [14]

$$F_D = \frac{1}{2} \rho C_D A_v^2 \quad (2.25)$$

Where ρ is the surrounding fluid density, A is the reference area (propeller cross-section, not area swept out by the propeller), and C_D is a dimensionless constant. This, while only accurate in some cases, is good enough for our purposes. This implies that the torque due to drag is given by [10]

$$\tau_D = \frac{1}{2} R \rho C_D A_v^2 = \frac{1}{2} R \rho C_D A (\omega R)^2 = b \omega^2 \quad (2.26)$$

Where ω is the angular velocity of the propeller, R is the radius of the propeller, and b is some appropriately dimensioned constant. [10]

Therefore total torque about body z axis is

$$\tau_Z = b \omega^2 + I_M \dot{\omega} \quad (2.27)$$

Now since $\dot{\omega}$ is very small compared to drag term, we ignore it, giving us the torques in body frame of reference as follows

$$\tau_b = \begin{bmatrix} Lk(\omega_1^2 - \omega_3^2) \\ Lk(\omega_4^2 - \omega_2^2) \\ b(\omega_1^2 + \omega_2^2 + \omega_3^2 + \omega_4^2) \end{bmatrix} \quad (2.28)$$

2.3.5 Equations of Motion

Rewriting what we have so far $x, y, z, \phi, \theta, \psi$ are the linear and angular positions in the Inertial frame

$\dot{x}, \dot{y}, \dot{z}$ are the linear velocities in the Inertial frame

$\omega_x, \omega_y, \omega_z$ are the angular velocities in the Body frame

$\omega_1^2, \omega_2^2, \omega_3^2, \omega_4^2$ are the squares of the rotor angular velocities of the Quadcoptor

$L, k, b, k_d, I_x, I_y, I_z$ are constants of the Quadcoptor and environment

W^{-1} is the inverted Wronskian Matrix defined in the earlier sections

$$\begin{bmatrix} \dot{\phi} \\ \dot{\theta} \\ \dot{\psi} \end{bmatrix} = W^{-1} \begin{bmatrix} \omega_x \\ \omega_y \\ \omega_z \end{bmatrix} \quad (2.29)$$

$$ThrustForceT_b = k \begin{bmatrix} 0 \\ 0 \\ \omega_1^2 + \omega_2^2 + \omega_3^2 + \omega_4^2 \end{bmatrix} \quad (2.30)$$

$$DragForceF_D = \begin{bmatrix} -k_d \dot{x} \\ -k_d \dot{y} \\ -k_d \dot{z} \end{bmatrix} \quad (2.31)$$

$$Torques\tau_b = \begin{bmatrix} Lk(\omega_1^2 - \omega_3^2) \\ Lk(\omega_4^2 - \omega_2^2) \\ b(\omega_1^2 + \omega_2^2 + \omega_3^2 + \omega_4^2) \end{bmatrix} \quad (2.32)$$

From this we calculate a Rotation matrix called ${}^I_B R$

$${}^I_B R = \begin{bmatrix} c\theta c\psi & s\theta s\phi c\psi - s\psi c\phi & s\theta c\phi c\psi + s\psi s\phi \\ c\theta s\psi & s\theta s\phi s\psi + c\psi c\phi & s\theta c\phi s\psi - c\psi s\phi \\ -s\theta & c\theta s\phi & c\theta c\phi \end{bmatrix} \quad (2.33)$$

Now we define the states as

$$\begin{bmatrix} x_1 \\ x_2 \\ x_3 \\ x_4 \\ x_5 \\ x_6 \\ x_7 \\ x_8 \\ x_9 \\ x_{10} \\ x_{11} \\ x_{12} \end{bmatrix} = \begin{bmatrix} x \\ y \\ z \\ \phi \\ \theta \\ \psi \\ \dot{x} \\ \dot{y} \\ \dot{z} \\ \omega_x \\ \omega_y \\ \omega_z \end{bmatrix} \quad (2.34)$$

Now using the Equations Derived above the Equations of motion in state space form are

$$\dot{x}_1 = x_7 \quad (2.35)$$

$$\dot{x}_2 = x_8 \quad (2.36)$$

$$\dot{x}_3 = x_9 \quad (2.37)$$

$$\begin{bmatrix} \dot{x}_4 \\ \dot{x}_5 \\ \dot{x}_6 \end{bmatrix} = W^{-1} \begin{bmatrix} x_{10} \\ x_{12} \\ x_{13} \end{bmatrix} \quad (2.38)$$

$$\begin{bmatrix} \dot{x}_7 \\ \dot{x}_8 \\ \dot{x}_9 \end{bmatrix} = \begin{bmatrix} 0 \\ 0 \\ g \end{bmatrix} + \frac{1}{m} ({^I_B}R\tau_b) + F_D \quad (2.39)$$

$$\begin{bmatrix} \dot{x}_{10} \\ \dot{x}_{11} \\ \dot{x}_{12} \end{bmatrix} = \begin{bmatrix} I_x^{-1} & 0 & 0 \\ 0 & I_y^{-1} & 0 \\ 0 & 0 & I_z^{-1} \end{bmatrix} \tau_b + \begin{bmatrix} \frac{I_z - I_y}{I_x} x_{11} x_{12} \\ \frac{I_x - I_z}{I_y} x_{10} x_{12} \\ \frac{I_y - I_x}{I_z} x_{11} x_{10} \end{bmatrix} \quad (2.40)$$

So these 12 are the total Equations of Motion

The model we've derived so far is highly simplified. We ignore a multitude of advanced effects that contribute to the highly nonlinear dynamics of a Quadcopter. We ignore rotational drag forces (our rotational velocities are relatively low), blade flapping (deformation of propeller blades due to high velocities and flexible materials), surrounding fluid velocities (wind), etc. [5]

2.4 Quadcopter Simulation

Now that we have complete equations of motion describing the dynamics of the system, we can create a simulation environment in which to test and view the results of various inputs and controllers. Although more advanced methods are available, we can quickly write a simulator which utilizes Euler's method for solving differential equations to evolve the system state. In MATLAB, this simulator would be written as follows. [5]

The functions and display code can be found in the appendix

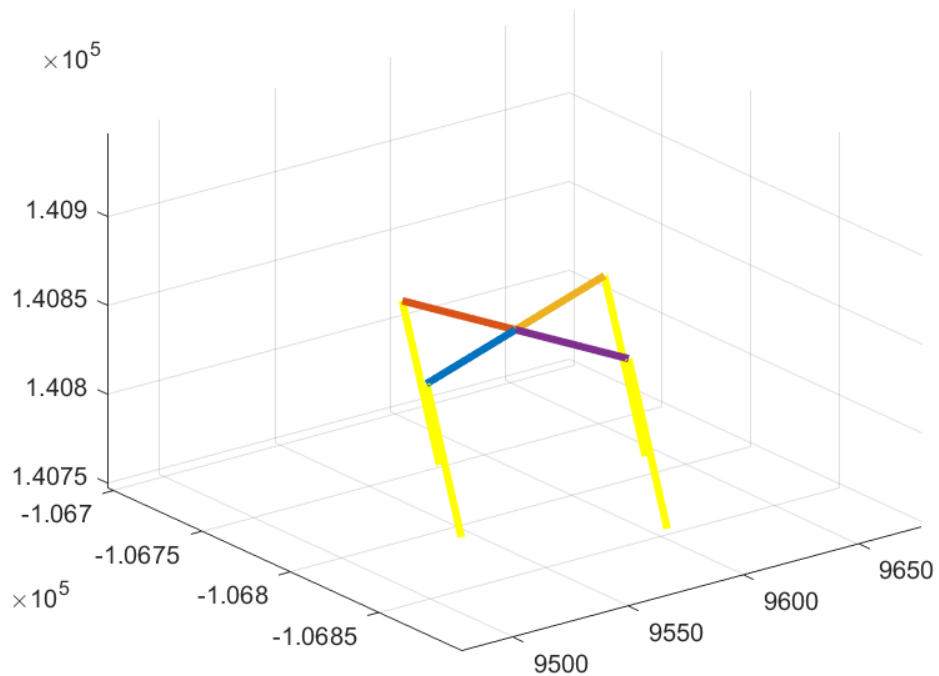


Figure 2.4: Simulation of Quadcopter motion

2.5 Quadcopter Control

The Quadcopter is an under - actuated system, meaning that it is impossible to control all the states independently of each other. So, in order to control the position in space we couple the rotations around x and y with accelerations in y and x axis.

For small angular rotations $\cos \theta = 1$, and $\sin \theta = \theta$

$${}^I_B R = \begin{bmatrix} c\theta c\psi & s\theta s\phi c\psi - s\psi c\phi & s\theta c\phi c\psi + s\psi s\phi \\ c\theta s\psi & s\theta s\phi s\psi + c\psi c\phi & s\theta c\phi s\psi - c\psi s\phi \\ -s\theta & c\theta s\phi & c\theta c\phi \end{bmatrix} \quad (2.41)$$

Becomes

$${}^I_B R = \begin{bmatrix} 1 & \theta\phi & \theta\phi \\ 0 & 1 & \phi \\ -\theta & \phi & 1 \end{bmatrix} \quad (2.42)$$

$$\begin{bmatrix} \dot{x}_7 \\ \dot{x}_8 \\ \dot{x}_9 \end{bmatrix} = \begin{bmatrix} 0 \\ 0 \\ g \end{bmatrix} + \frac{1}{m}({}^I_B R \tau_b) + F_D \quad (2.43)$$

Acceleration in x is dependent on rotation around x and rotation around y and

Acceleration in y is dependent only on rotation around x.

Thus in effect if we can maintain the angles around x and y at zero then we can maintain the acceleration in x and y at zero.

So we create a control input in order to maintain the angles to zero assuming error to be the (angle - zero) = angle

$$Torques \tau_b = \begin{bmatrix} Lk(\omega_1^2 - \omega_3^2) \\ Lk(\omega_4^2 - \omega_2^2) \\ b(\omega_1^2 + \omega_2^2 + \omega_3^2 + \omega_4^2) \end{bmatrix} \quad (2.44)$$

$$\begin{bmatrix} \dot{x}_{10} \\ \dot{x}_{11} \\ \dot{x}_{12} \end{bmatrix} = \begin{bmatrix} I_x^{-1} & 0 & 0 \\ 0 & I_y^{-1} & 0 \\ 0 & 0 & I_z^{-1} \end{bmatrix} \tau_b + \begin{bmatrix} \frac{I_z - I_y}{I_x} x_{11} x_{12} \\ \frac{I_x - I_z}{I_y} x_{10} x_{12} \\ \frac{I_y - I_x}{I_z} x_{11} x_{10} \end{bmatrix} \quad (2.45)$$

Therefore to create angular acceleration in opposite direction to existing rotation in x direction we see that the inputs should be as follows

$$\omega_1^2 = -K_p(\theta) \quad (2.46)$$

$$\omega_3^2 = K_p(\theta) \quad (2.47)$$

Where K_p is the proportionality constant

Similarly for adding a differential term,

$$\omega_1^2 = -K_p(\theta) - K_d \left(\frac{d\theta}{dt} \right) \quad (2.48)$$

$$\omega_3^2 = +K_p(\theta) + K_d \left(\frac{d\theta}{dt} \right) \quad (2.49)$$

Similarly for y axis

$$\omega_2^2 = +K_p(\phi) - K_d \left(\frac{d\phi}{dt} \right) \quad (2.50)$$

$$\omega_4^2 = -K_p(\phi) - K_d \left(\frac{d\phi}{dt} \right) \quad (2.51)$$

For z axis

$$\omega_1^2 = -K_p(\psi) - K_d \left(\frac{d\psi}{dt} \right) \quad (2.52)$$

$$\omega_2^2 = -K_p(\psi) - K_d \left(\frac{d\psi}{dt} \right) \quad (2.53)$$

$$\omega_3^2 = -K_p(\psi) - K_d \left(\frac{d\psi}{dt} \right) \quad (2.54)$$

$$\omega_4^2 = -K_p(\psi) - K_d \left(\frac{d\psi}{dt} \right) \quad (2.55)$$

Also in order to balance gravity, the total thrust in global z axis should be mg.

That implies

$$mg = \cos\theta \cos\phi k (\omega_1^2 + \omega_2^2 + \omega_3^2 + \omega_4^2) \quad (2.56)$$

In stable condition each rotor will take equal weight resulting in the following equations to balance gravity

$$\omega_1^2 = \frac{mg}{4k \cos\theta \cos\phi} \quad (2.57)$$

$$\omega_2^2 = \frac{mg}{4k \cos\theta \cos\phi} \quad (2.58)$$

$$\omega_3^2 = \frac{mg}{4k \cos\theta \cos\phi} \quad (2.59)$$

$$\omega_4^2 = \frac{mg}{4k \cos\theta \cos\phi} \quad (2.60)$$

Thus we have all the equations for the final PD controller, combining them we have the equations for the inputs as follows

$$\omega_1^2 = \frac{mg}{4k \cos\theta \cos\phi} - K_p(\psi) - K_d \left(\frac{d\psi}{dt} \right) - K_p(\theta) - K_d \left(\frac{d\theta}{dt} \right) \quad (2.61)$$

$$\omega_1^2 = \frac{mg}{4k \cos\theta \cos\phi} - K_p(\psi) - K_d \left(\frac{d\psi}{dt} \right) + K_p(\phi) + K_d \left(\frac{d\phi}{dt} \right) \quad (2.62)$$

$$\omega_1^2 = \frac{mg}{4k \cos\theta \cos\phi} - K_p(\psi) - K_d \left(\frac{d\psi}{dt} \right) + K_p(\theta) + K_d \left(\frac{d\theta}{dt} \right) \quad (2.63)$$

$$\omega_1^2 = \frac{mg}{4k\cos\theta\cos\phi} - K_p(\psi) - K_d \left(\frac{d\psi}{dt} \right) - K_p(\phi) - K_d \left(\frac{d\phi}{dt} \right) \quad (2.64)$$

This Controller was implemented and results were compared with a similar simulation done in [5]. The controller gains were found by trial and error approach until the results matched the ones given in [5].

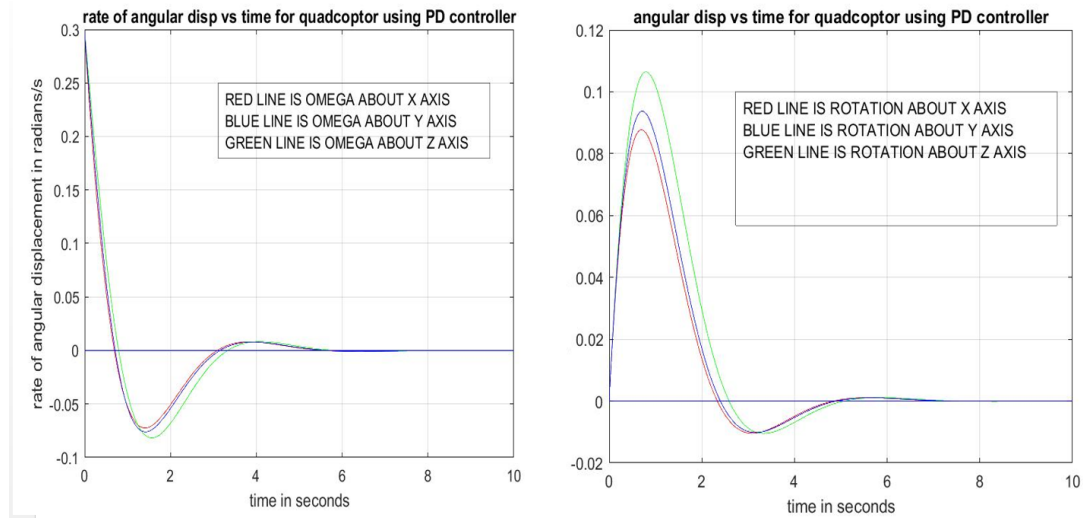


Figure 2.5: Angular Deflection vs. Time I& Angular Velocity vs. time -MATLAB simulation

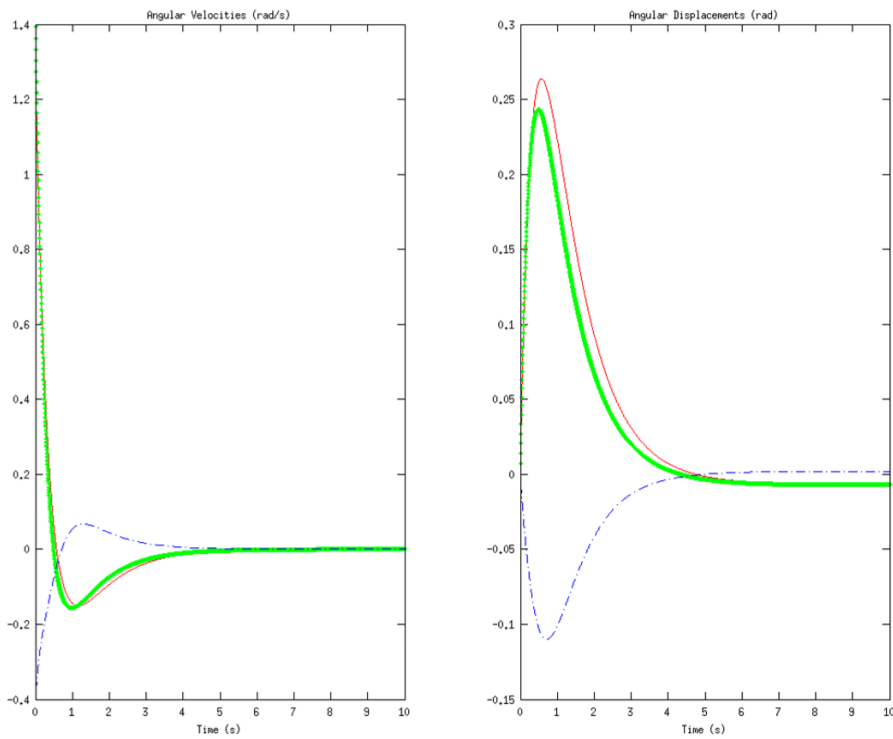


Figure 2.6: Angular Deflection vs. Time I& Angular Velocity vs. time –Reference Paper [5]

Comparing figures 8 and 9 we can see that the controller in [5] is critically damped in nature and there are no oscillations visible. In Figure 8 there are visible oscillations indicating that the system is underdamped.

The overall behavior of the two controllers is the same and the difference in overshoot and settling time are mainly attributable to the consistency in the initial value of the constants like mass, moment of inertia etc.

2.6 Recoil Modelling

Average Recoil force on the Trunnion (Standard Units) is given by. The Trunnion is the hinge on which the primary barrel of the gun is pivoted on.

$$F = (wP \times vP + wC \times vC)^2 / (2 \times g \times wG \times L) \quad (2.65)$$

F = Force on Trunnion

wP = Weight of Projectile

wC = Weight of Propellant

wG = Weight of recoiling mass of the gun

vP = Muzzle velocity of projectile

vC = Escape Velocity of Propellant Gasses

L = Length of Recoil

g = Acceleration due to gravity

After which the projectile executes a projectile motion. The PLD selected for this simulation is the 0.32" ASHANI MARK -II Pistol [6].

0.32" ASHANI MARK -II Pistol

TECHNICAL SPECIFICATION:-	
	Caliber : 0.32"
	Barrel length : 91.44mm
	Magazine : Box type (capacity-08 rounds)
	Weight : 680 grams
	Range : 18.27 meters
	Action : Semi automatic (blow back)
	Replacement of magazine : Quick release mechanism (Push button)
	Hammer position : Exposed
	Grip : Full Wooden/Polymer Grip with GSF metallic logo
	Safety : Four Types
	Dimentions : 163 X 111 X 38 (mm)

Figure 2.7: Ashani Mark – II Pistol – Made in India [6]

This gun has an effective range of 18 meters and a muzzle velocity of 300m/s. From this we can calculate the bullet will reach the target in 0.06 seconds and the bullet will sink by 17.658 millimeters.

This is very low, and for all practical accuracy purposes it can be considered that the bullet will travel in a straight line.

Therefore the important parameters are

Time taken by bullet in barrel = 0.00059285 seconds (Barrel Time)

Max Range = 18 meters (Range)

Max time of flight = 0.06 seconds (Time till impact)

Max drop in height due to projectile motion = 17.658 millimeters

Thus the control problem for a PLD mounted Quadcopter can be divided into two parts

1. The issue of angular deviation in the short time of 0.00059285 seconds
2. The time taken by the Quadcopter to return to stable position in order to shoot again

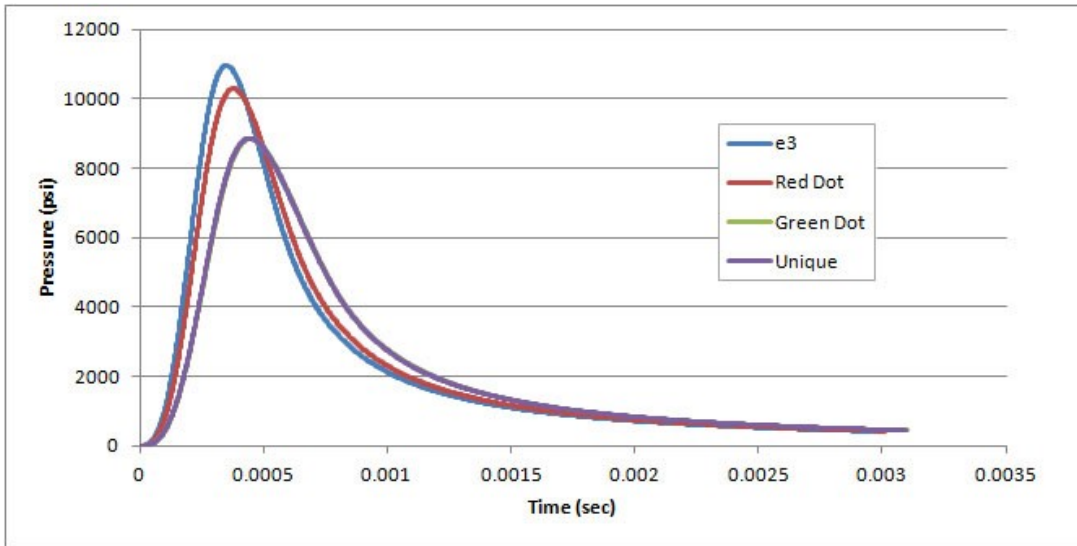


Figure 2.8: Pressure vs Time of ASHANI MARK -II Pistol [6]

Summary

In this Chapter, the standard method for modelling and controlling Quadcoptors was studied. This method was used to create a MATLAB model on which a basic PD controller was applied. The behaviour of the model was compared with the results provided in REF. and the behaviour was found to match.

The recoil of a handgun was modelled for further inclusion in the complete model of a Multi-rotor UCAV.

Chapter 3

Effect of Control Gains on Stability of a PLD mounted Quadcoptor

3.1 Models Considered

3.1.1 6 DOF Planar System

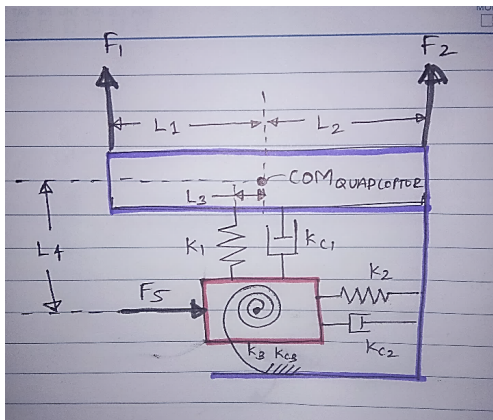


Figure 3.1: Six DOF planar Model



Figure 3.2: UCAV by Duke Robotics

[3]

The Six DOF model is one in which the PLD is connected to the Quadcopter frame with springs and Dampers in X, Y and θ directions. The Location of the PLD with respect to the Quadcopter COM is left variable by giving L1, L2 and L3 as the Parameters.

The external Recoil force is modeled as a force acting in the positive X direction on the COM of the PLD. The Propeller thrusts are given by forces F1 and F2. The Propeller forces are pre decided according to the control algorithm and hence in this model they are not considered inputs.

The first mathematical model was made planar so as to reduce the degrees of freedom and simplify the problem. In a single plane the PLD is attached to the Quadcopter with individual springs and dampers in all three degrees of freedom. The location of the PLD's recoil vector with respect to the center of mass of the Quadcopter was also kept variable using the parameters L1, L2, L3 and L4.

The aim of this model was to simulate the behavior of the PLD mounted Quadcopter for some values of the parameters and some values of recoil. A control PD algorithm was pre-programmed into the Quadcopter mathematical model, thus the thrust force F1 and F2 were defined. So for this system the sole input was the recoil force F5.

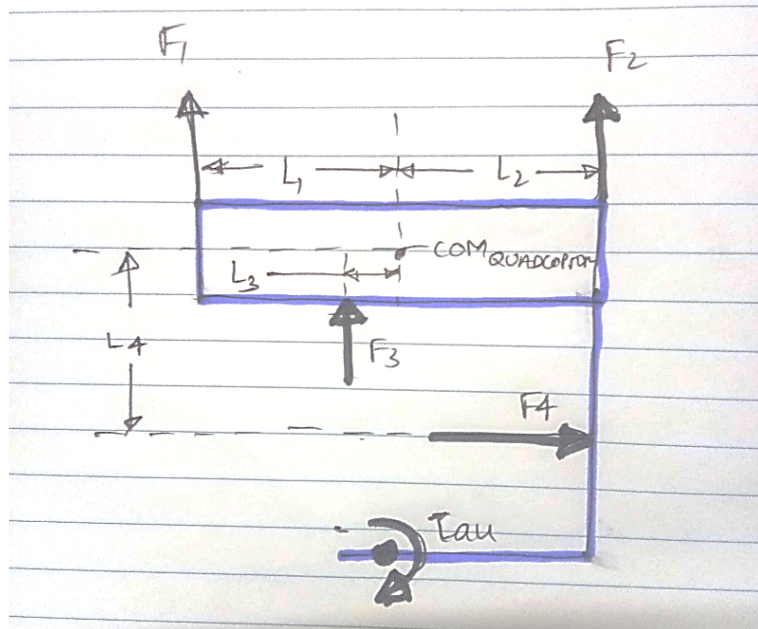


Figure 3.3: Free body diagram of the Quadcopter

The Equations of motion for the Quadcopter come to be

$$m_1 \ddot{x}_1 = -(F_1 + F_2 + F_3) \sin\theta + F_4 \cos\theta \quad (3.1)$$

$$m_1 \ddot{y}_1 = -m_1 g + (F_1 + F_2 + F_3) \cos\theta + F_4 \sin\theta \quad (3.2)$$

$$I_1 \ddot{\theta} = -F_1 L_1 + F_2 L_2 - F_3 L_3 + F_4 L_4 + \tau \quad (3.3)$$

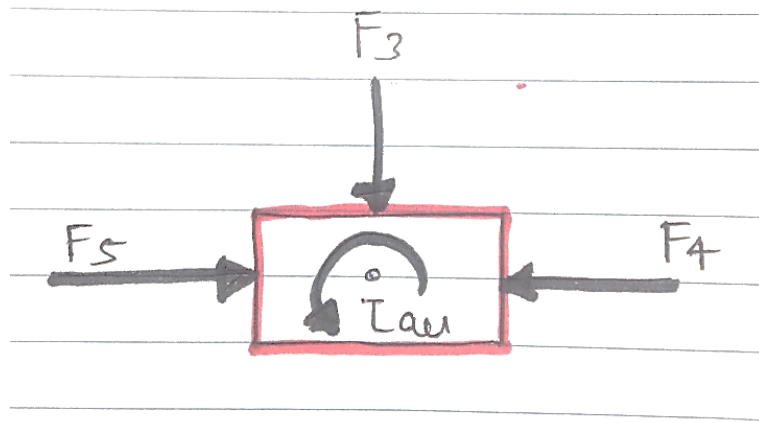


Figure 3.4: Free Body Diagram of the PLD

The Equations of motion for the PLD come to be

$$m_2 \ddot{x}_2 = F_5 \cos\phi - F_4 \cos\theta + F_3 \sin\theta \quad (3.4)$$

$$m_2 \ddot{y}_2 = -m_2 g + F_5 \sin\phi - F_4 \sin\theta - F_3 \cos\theta \quad (3.5)$$

$$I_2 \ddot{\phi} = -\tau \quad (3.6)$$

Where, F stands for Forces and subscript 1 stands for Quadcopter properties and subscript 2 stands for PLD properties, all other symbols have their usual meaning. Theta is the angle of the Quadcopter with the Inertial frame of reference and phi is the angle of

the PLD with the Inertial Frame of Reference.

This planar model is sufficient to capture the major effects of recoil on a Quadcopter, and the results can be used to make valid assumptions on the behavior of the real system. An issue that is definitely not addressed in this model is the anti-torque due to rifling present in many projectile launching devices.

The control equations of this model are entirely the same as the full Quadcopter model, but with less no. of states. The control is completely independent of the angle of the projectile launching device or its position in the plane.

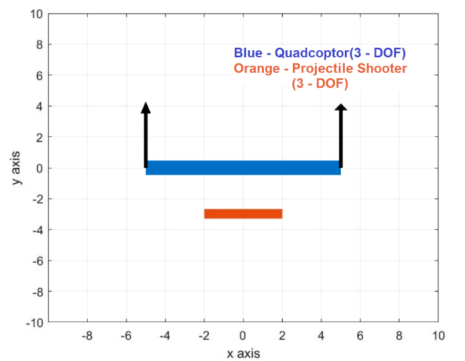


Figure 3.5: Simulation of the Six DOF model - 1

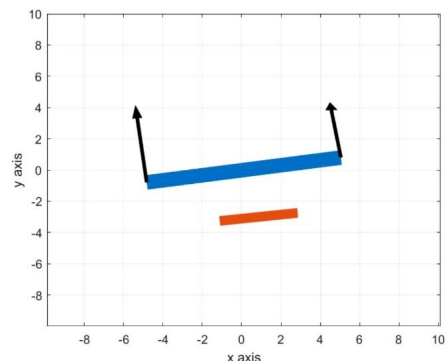


Figure 3.6: Simulation of the Six DOF model - 2

The modelling was done on MATLAB and the differential equation solver used was ODE45. The results were also simulated so as to provide better intuitive understanding as to the effect of the recoil.

Figure 15 shows the PLD mounted Quadcopter in its initial state and figure 16 shows it after the recoil has been applied. The length of the black arrows show the thrust produced by the two propellers.

Using this MATLAB code, the behavior of the Quadcopter and the projectile launch-

ing device was observed for various inputs F5.

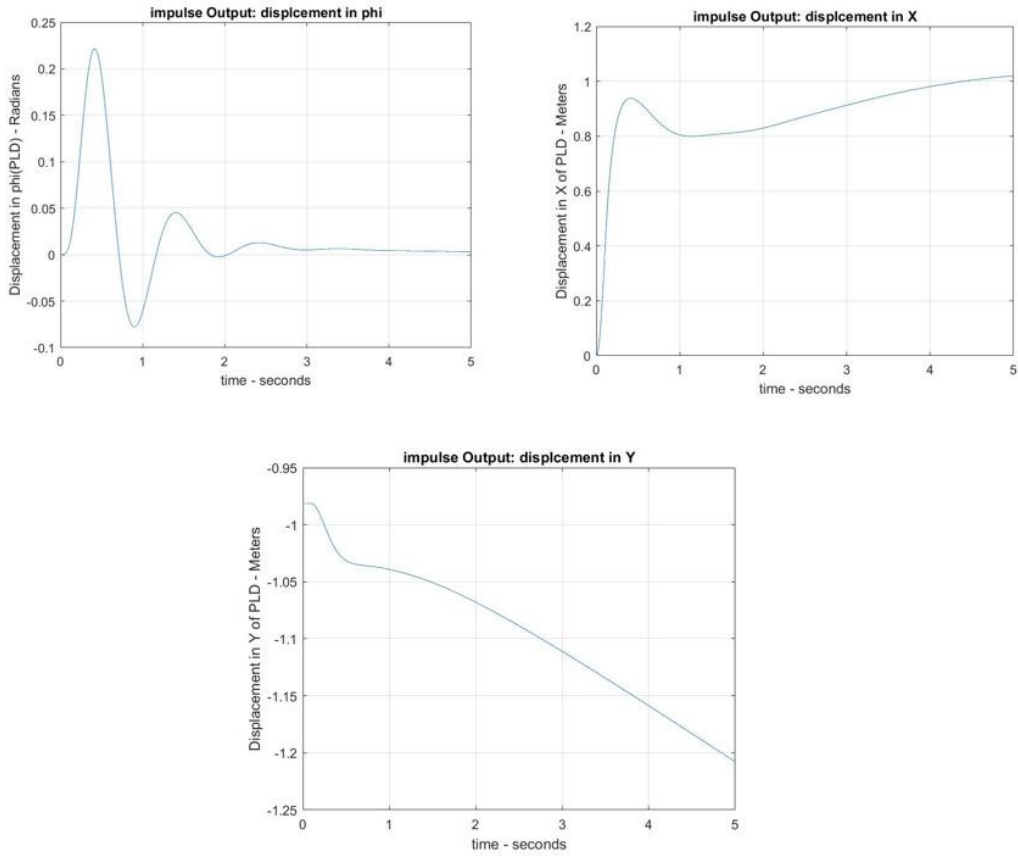


Figure 3.7: Variation of the PLD states namely x_2, y_2 and ϕ with time

The PD controller implemented in the code only accounted for stabilizing the angle (ϕ) of the Quadcopter and not the elevation or the lateral position (x_2, y_2). This results in a drift in the 2 – non controlled states. Also this model proves that there is a need to monitor all the states as well as the need for an integrator term in the control equation to neutralize the drift.

3.1.2 Three DOF Model

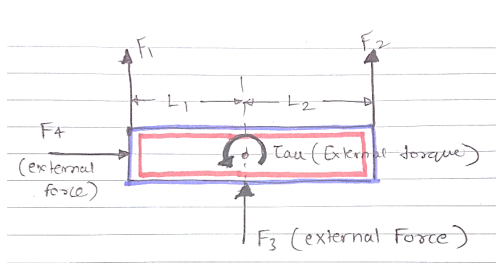


Figure 3.8: Three DOF MATLAB model



Figure 3.9: A DIY Gun mounted Quadcopter [7]

The Three DOF model is one in which the PLD is connected to the Quadcopter frame rigidly. The external Recoil force is modeled as a forces acting in the positive X direction (F_4), Y direction (F_3) on the COM and a torque (τ). This is done in order to more clearly understand the impacts of each component on the behavior of the PLD mounted Quadcopter. The Propeller thrusts are given by forces F_1 and F_2 . The Propeller forces are pre decided according to the control algorithm and hence in this model they are not considered inputs.

In this model the Projectile Launching Device is rigidly attached to the Quadcopter. This model is thus simpler than the previous model. This design is also very popular with the DIY community of drone enthusiasts.

The Equations of motion are as follows

$$m_1 \ddot{x}_1 = -(F_1 + F_2 + F_3) \sin\theta + F_4 \cos\theta \quad (3.7)$$

$$m_1 \ddot{y}_1 = -m_1 g + (F_1 + F_2 + F_3) \cos\theta + F_4 \sin\theta \quad (3.8)$$

$$I_1 \ddot{\theta} = -F_1 L_1 + F_2 L_2 + \tau \quad (3.9)$$

Where F_3 , F_4 and τ are the external forces and torques applied to the Quadcopter due to recoil. All other symbols have similar meanings to that in the previous model. This arrangement of separating out the coupled nature of the torque and the force due to recoil is deliberate. This allows one to analyze the effect of each of the components of the recoil force and what impact it has on the behavior of the Quadcopter.

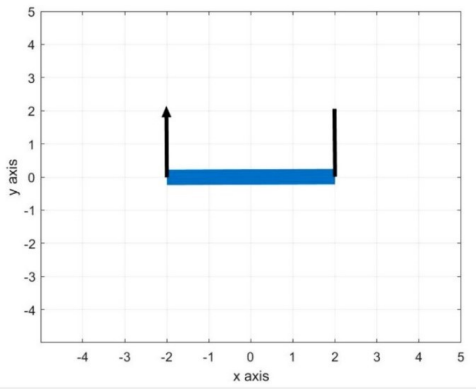


Figure 3.10: Three DOF MATLAB model

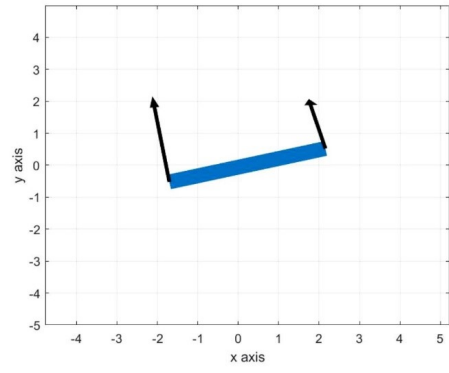


Figure 3.11: Simulation of Three DOF Model

The control equations used are the same as described in the literature review and the system goes back to equilibrium in all cases. Initially the model was given impulses in individual directions of x , y and θ and the result was simulated. In order to test the sensitivity of the Quadcopter to different inputs, the model was linearized and impulse response of individual inputs to individual outputs was found.

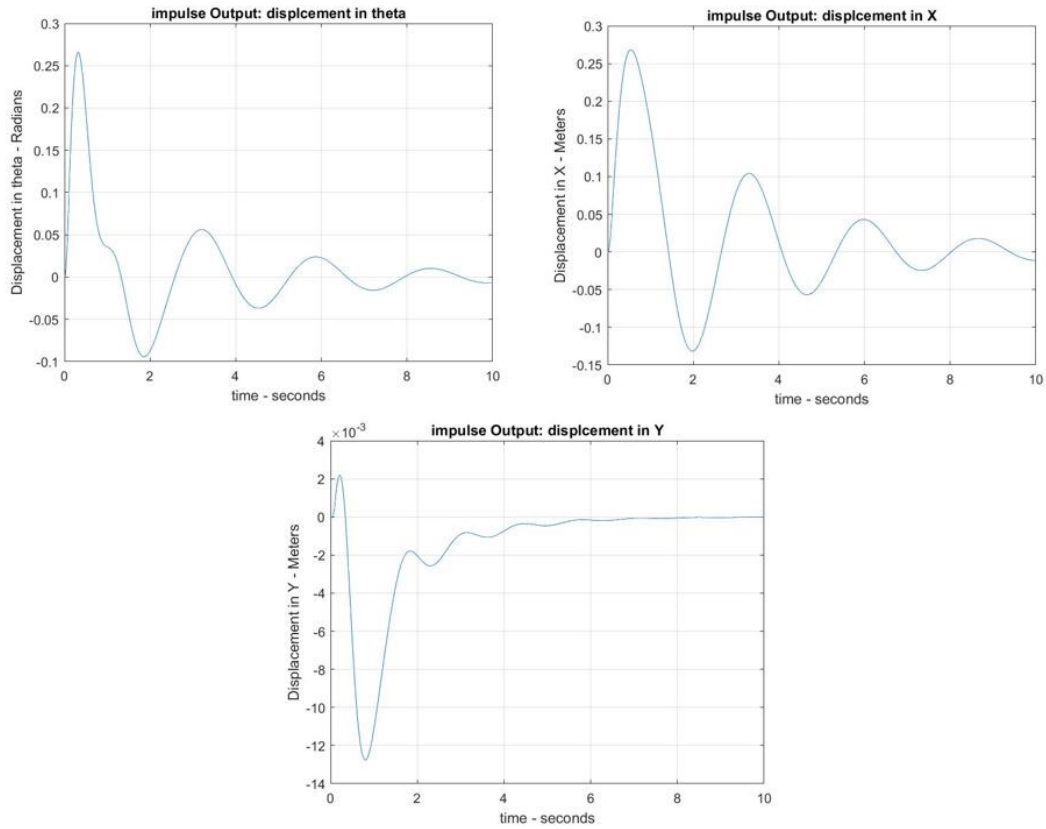


Figure 3.12: Simulation Results of the Three DOF model

Figure 22 shows that the system returns to the equilibrium point in all cases, hence, the implemented control system is convergent, but not yet optimized.

Where In(1) is F_3 , In(2) is F_4 and In(3) is τ .

And Out(1) is X displacement, Out(2) is Y displacement and Out(3) is Theta Displacement.

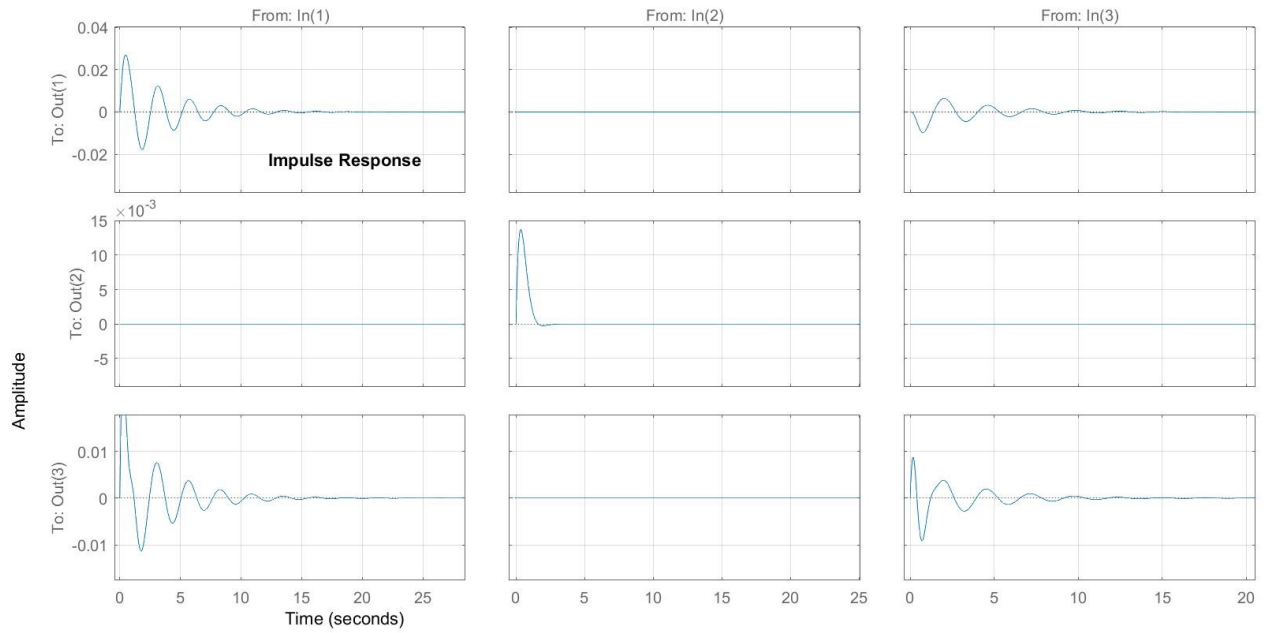


Figure 3.13: Impulse Response of the Three DOF model

As is clearly visible from the figure 23, The In(2) is the one and only factor affecting Out(2) thus they have a one to one co-relation while the other input-outputs are coupled.

From the Figure 23, it is clear that the three DOF model behaves like a spring mass system in the Y – direction.

3.2 Methodology for tuning controller gains using spring mass Damper analogy

The basis for this methodology is the underlying assumption that “The Behavior of the Quadcopter to inputs is analogues to the behavior of a second order spring mass damper system”. This assumption has some basis in the fact that the impulse response of the Quadcopter system closely matches with that of a second order system. The Transfer function of the linearized system of the PLD mounted Quadcopter is 6th order in nature but by observing the coefficients we can conclude that the behavior can be closely approximated by a 2nd order Transfer function as well.

```
Input: theta angular impulse Output: displacement in X

ans =

```

$$\frac{0.1 s^4 + 0.4905 s^3 + 0.981 s^2}{s^6 + 9.905 s^5 + 84.34 s^4 + 343.4 s^3 + 976.3 s^2 + 1684 s + 2406}$$

Figure 3.14: 6_{th} order Transfer function of the linearized three DOF mode

This is useful as there are established ways of designing optimal spring-damper base structures for a projectile launching device.

The standard second order transfer function is

$$\frac{\omega_n^2}{s^2 + 2\zeta\omega_n s + \omega_n^2} \quad (3.10)$$

Using a gain value in multiplication with the TF allows for an approximate fit.

So the methodology to port the optimal spring mass damper design to controller gain Design goes as follows.

Step 1. Fit second order responses on top of the existing impulse responses using logarithmic decrement and frequency plotting

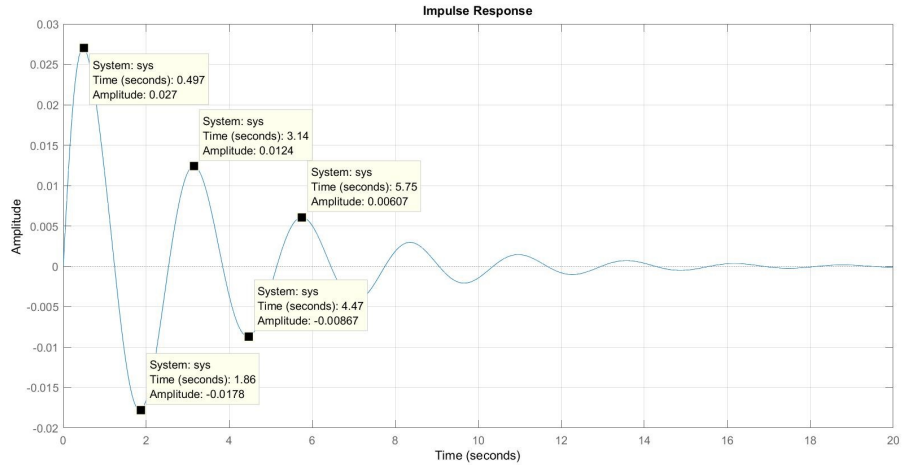


Figure 3.15: Crests and troughs of the Impulse response of the Three DOF Model

Step 2. Using these find values of frequency and damping coefficient (ζ) corresponding to the gains of the control equation. The frequency and ζ can also be represented by a spring stiffness and a damping factor.

Step 3. Change the control gains and repeat steps 1 and 2 to form a table of control equation gains vs. their corresponding spring stiffness's and damping factor.

Step 4. Find an empirical relationship between the control gains and the spring/damper values.

Step 5. Use the established method of critical damping to find optimized values of spring stiffness and damping coefficient.

Step 6. Using the empirical relationship found in step 4, find optimal control gains for the Quadcopter with a PLD.

The Variation of the Damping ratio and Frequency of oscillations with various K_p and K_d values is as follows

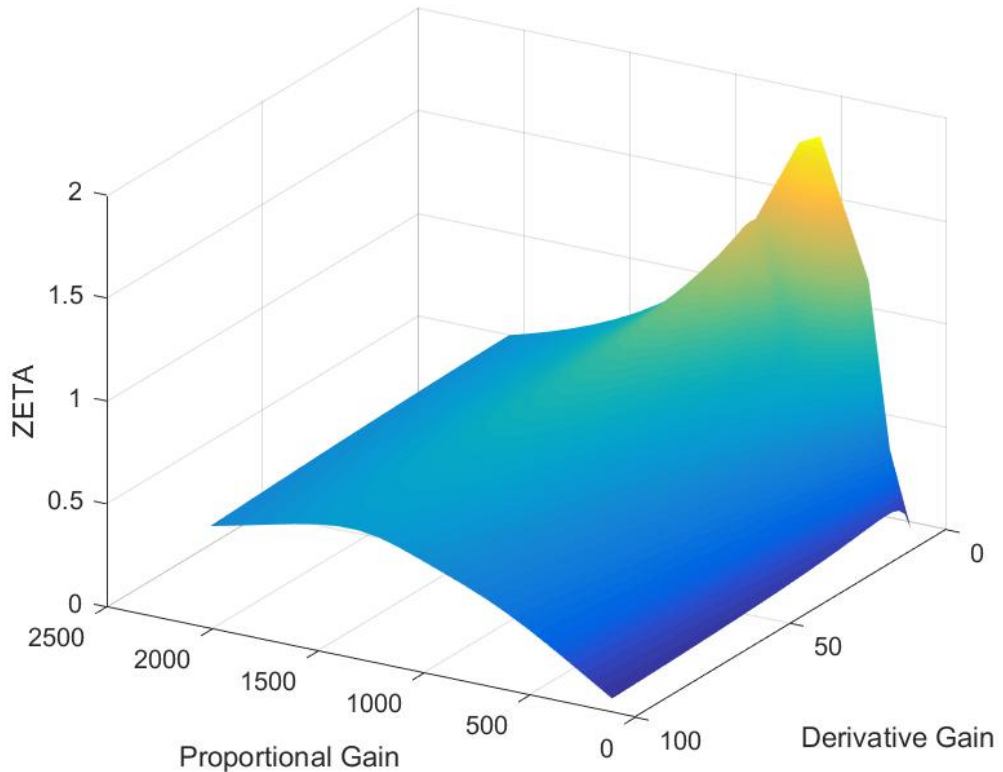


Figure 3.16: Variation of Zeta with Proportional Gain and Derivative Gain

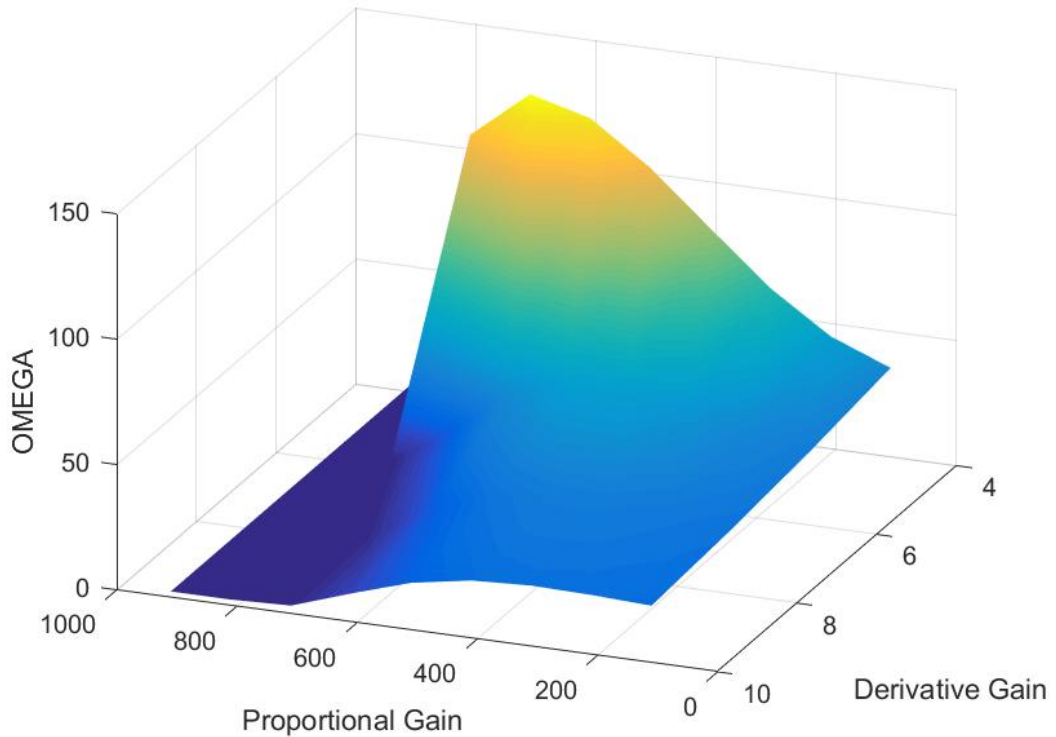


Figure 3.17: Variation of Damped oscillation frequency ω_d with Proportional Gain and Derivative Gain

With this information, we get a value for the initial proportional and derivative gains for the controller tuning procedure.

Summary

In this chapter 2 models were proposed to simulate the behaviour of a Quadcopter UCAV, a 3 DOF planar model and a 6 DOF planar model. In the 6 DOF model, the Gun was not attached to the Quadcopter rigidly, but was coupled with linear and torsional spring/damper elements. In the 3 DOF model the Gun was rigidly attached to the Quadcopter. The algorithm for these models was implemented in MATLAB.

A method for tuning Control Gains used in artillery base structures, which uses the analogy of spring-mass-damper system was used to find the gains which resulted in a

”Critically Damped” Behaviour of the system.

Chapter 4

Experimental Setup

In order to check the effect of the control strategies on the accuracy and firing rate of the PLD mounted Quadcopter, it is necessary to create an Experimental setup that allows the measurement of the accuracy and firing rate.

The experimental setups considered were as follows—

1. Full Quadcopter with PLD
2. Full Quadcopter with a small impulse causing device (*to check Quadcopter stability etc.*)
3. 2D Equivalent of a Quadcopter with a PLD (*to check both accuracy/precision and Quadcopter behavior*)

Out of the three possible setups, due to time limitations, the third option was selected to be built.

4.1 SolidWorks Model of the Setup

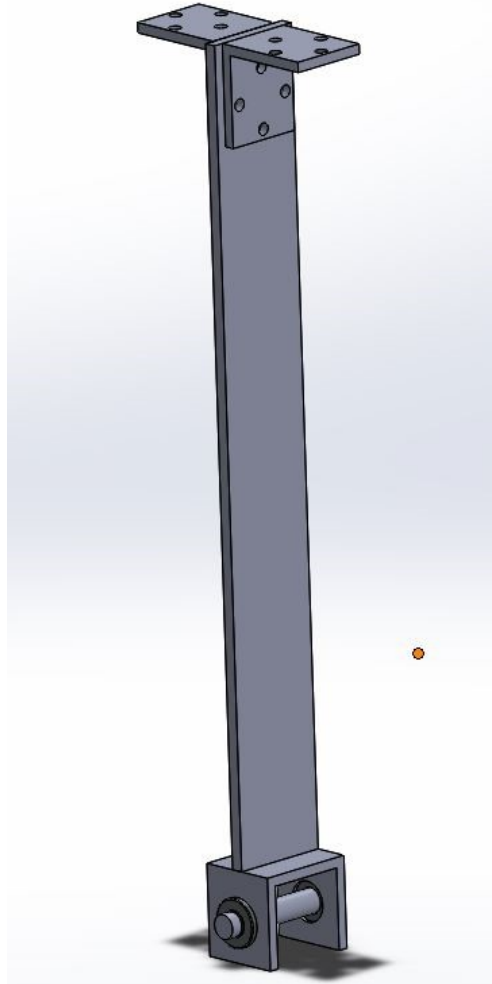


Figure 4.1: Long Cantilever Type



Figure 4.2: Paeucelliers Mechanism Type

Two Possible models were considered for the 2D equivalent design

- 1. Long Cantilever Type** This model uses a long cantilever to generate approximate straight line motion and a Pivot at the end for rotational freedom.

This model has the advantages of being simple and robust with minimum no. of joints. The only disadvantage is the approximate straight line motion and the stiffness

of the cantilever exerting some extra forces on the Quadcoptor

2. Paeucelliers Mechanism Type This model uses a Paeucelliers mechanism to generate exact straight line motion and a Pivot at the end for rotational freedom.

This model has the disadvantages of being Complex and Fragile with many binary and ternary joints. The advantage is the exact straight line motion the model generates.

Considering the limitations of time and the robustness offered by the cantilever design, this design was selected. In order to sense the amount of impulse generated by the gun on the setup, a strain gauge will be attached to the flat face of the top part of the cantilever (where the stress is the maximum).



Figure 4.3: Cross Section of Cantilever



Figure 4.4: Cantilever Beam

4.2 Gun Selection

In order to most accurately simulate the effects of a real gun, without using a real gun (as the procedure for obtaining a gun license for academic use is lengthy and cumbersome), several options were explored –

1. Toy Gun
2. Air Gun with Long Barrel – High Recoil
3. Air Gun with Short Barrel – lower Recoil
4. Custom spring Based shooting device



Figure 4.5: Toy Gun



Figure 4.6: Toy Shotgun



Figure 4.7: Air Gun

4.2.1 Gun Actuation Mechanisms

For actuating the Gun while on the Quadcopter, two mechanisms were considered.

1. Linear Actuator coupled to the trigger



Figure 4.8: Linear Actuator



Figure 4.9: Linear Actuator Coupled With Trigger

2. Rotary Actuator with a steel String tied to the Trigger.



Figure 4.10: Motor with Steel String attached to The Trigger - 1



Figure 4.11: Motor with Steel String attached to The Trigger - 2

4.3 Quadcopter Size Selection

In order to see the effects of the gun recoil on the stability of the Quadcopter, the two must be of comparable masses. If the mass of the Quadcopter is too large, the effects seen will be negligible, and the experiment would become unrealistic. If the Quadcopter is too small, it will be unable to stabilize the effects of the recoil and the experiment would be again unsuccessful.

The Power rating of BLDC motors – most commonly used motors in Quadcopters – is in Kilo – Volt – Amperes. The Options available were

1. Custom Quadcopter Frame and Standard BLDC motors of Required Rating
2. Standard Quadcopter Frame with BLDC motors of rating of 2200 KVA

Since the Standard Quadcopter frame and motors were within the range of acceptable size constraints of the setup, The Standard Quadcopter was selected



Figure 4.12: 2D Quadcoptor

4.4 Mathematical Model and Simulation in MATLAB of the Experimental Setup

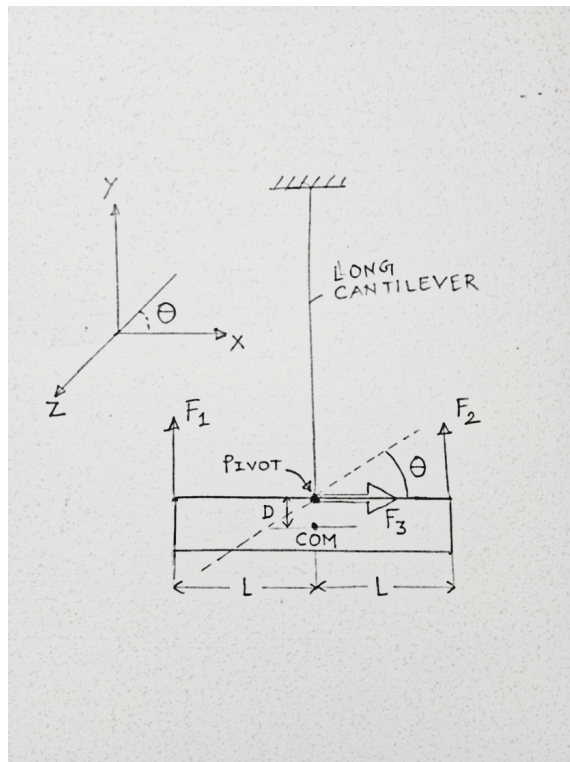


Figure 4.13: EOM with out Gun

First a mathematical model for the 2D Quadcopter was constructed in order to verify the behavior of the model vs. the actual Setup.

The constants are

1. M - Equivalent Sprung Mass of the Quadcoptor + Cantilever
2. I - Moment of Inertia of the Quadcoptor about its COM

Equations of Motion are

$$\ddot{x} = \frac{1}{M} [F_3 - (F_1 + F_2)\sin\theta] \quad (4.1)$$

$$\ddot{\theta} = \frac{1}{M} [-F_3 D - (F_1 - F_2)L - MgD\sin\theta] \quad (4.2)$$

Assuming a Long Cantilever, the motion in y direction is negligible

$$\ddot{y} = 0 \quad (4.3)$$

For a small displacement, the force of the cantilever can be given by

$$F_3 = -kx \quad (4.4)$$

Where K is the Stiffness constant.

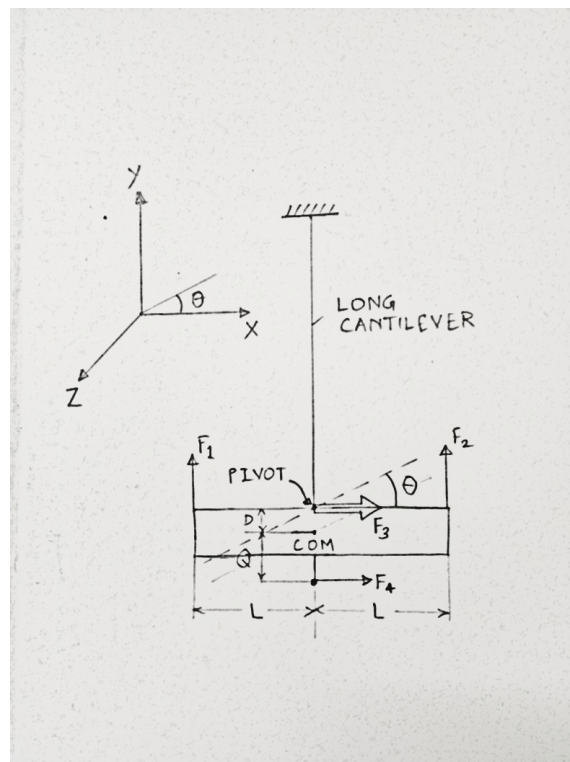


Figure 4.14: EOM with Gun

This is the complete 2 Dimensional mathematical model for a Quadcopter with a Gun. The added quantities are the force due to Recoil F_4 and the perpendicular distance between the COM and the barrel of the gun, 'Q'.

The Equations of the Motion are

$$\ddot{x} = \frac{1}{M} [F_3 + F_4 - (F_1 + F_2) \sin\theta] \quad (4.5)$$

$$\ddot{\theta} = \frac{1}{M} [-F_3 D + F_4 Q - (F_1 - F_2)L - MgD \sin\theta] \quad (4.6)$$

Assuming a Long Cantilever, the motion in y direction is negligible

$$\ddot{y} = 0 \quad (4.7)$$

For a small displacement, the force of the cantilever can be given by

$$F_3 = -kx \quad (4.8)$$

Where K is the Stiffness constant.

4.5 Full Setup



Figure 4.15: Full Setup 1



Figure 4.16: Full Setup 2

The experimental setup is used to implement various control strategies and see the effect on the accuracy, precision and firing rate of the gun. The long cantilever allows the movement of the Quadcoptor in a single plane. As the Quadcoptor is also mounted on a single pivot, it is free to rotate in the same plane. The gun is attached below

the Quadcoptor rigidly. This method of mounting the gun is not used currently, as the impulse is directly transmitted to the Quadcoptor, but this is the simplest method of mounting a gun and will establish a starting point to further development of mounting methods.

4.6 Mathematical Model Validation with actual setup

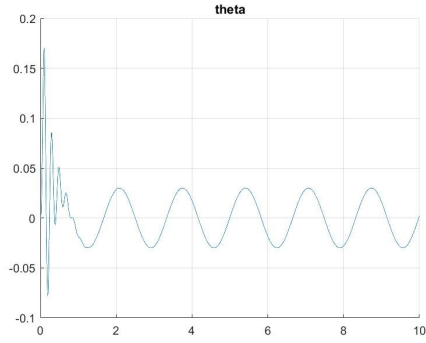


Figure 4.17: Angular Displacement (Theta) Vs. Time of the Mathematical Model

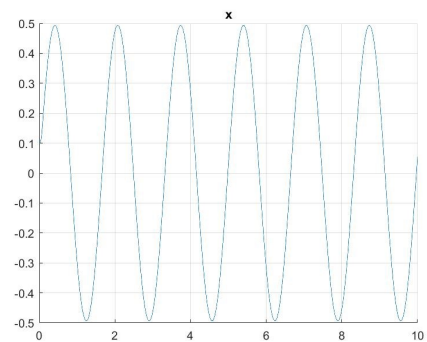


Figure 4.18: Linear Displacement (X) Vs. Time of the Mathematical Model

The Mathematical model was simulated and the Quadcopter was made to oscillate independently in the X and Theta directions. The output graphs were plotted for each. This data was compared to the actual setup's behavior.

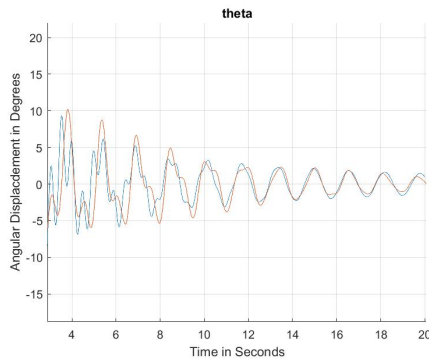


Figure 4.19: Angular Displacement (Theta) Vs. Time of the Mathematical Model(blue) and IMU values from the setup(red)

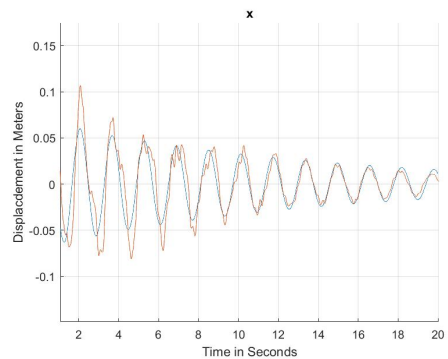


Figure 4.20: Linear Displacement (X) Vs. Time of the Mathematical Model(blue) and IMU values from the setup(red)

This validates the proposed Mathematical model.

4.7 Simulation to Obtain Control Gains

In order to Implement a controller onto the Experimental setup, it was first necessary to get an idea of which controller would be the most useful in minimizing ‘maximum overshoot’, ‘Rise Time’ and ‘settling time’.

Most basic commercial Quadcopters use a version of the Proportional Derivative controller in order to stabilize the states and achieve position and/or velocity control.

So the mathematical model was simulated using an impulse approximated by an inverted parabola.



Figure 4.21: Ashani Mark – II Pistol – Made in India [19] [6]

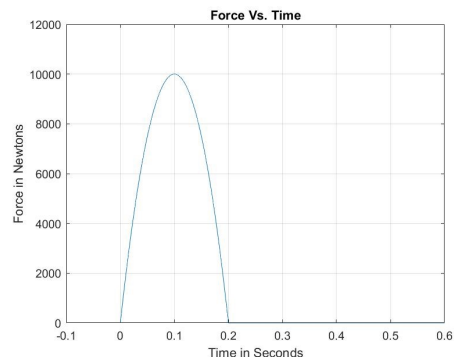


Figure 4.22: Recoil force used in Simulation to approximate the actual gun recoil

Using this approximation, the model was evolved and the resulting behaviour of the system was captured using plots and an animation. Using the initial value of control gains from the mathematical model developed in the previous section on control gains, we see that the behaviour is still nearly critically damped.

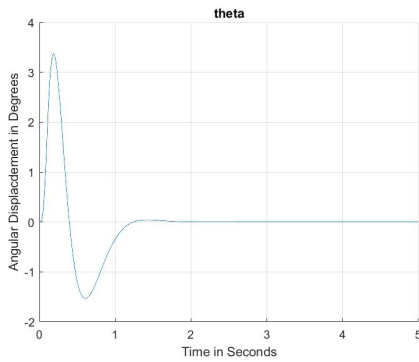


Figure 4.23: Simulated output of Theta Vs. time for a PD Controller

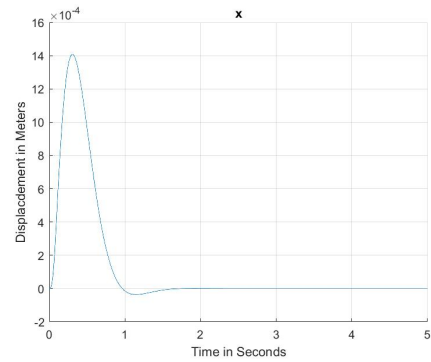


Figure 4.24: Simulated output of X Vs. time for a PD Controller

4.8 Sensors

The setup effectively has 2 degrees of freedom that require estimation. An Inertial Measurement Unit is a must for any multi-rotor, and in addition a strain gauge is placed onto the surface of the cantilever to infer the linear displacement of the Quadcopter without the Drift issues faced by IMU's.



Figure 4.25: Strain Gauge on Cantilever beam

The Strain Gauge measurements were extracted using a vishay strain gauge indicator model P3. The output of which was connected to the onboard Arduino in order to implement control.



Figure 4.26: vishay strain gauge indicator model P3

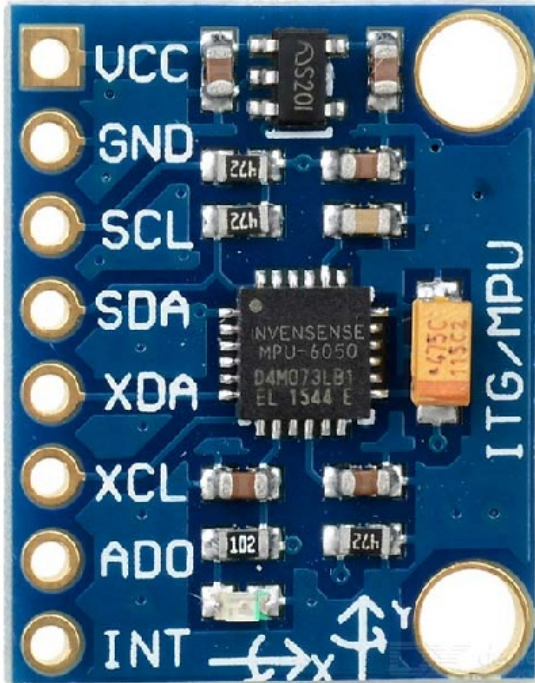


Figure 4.27: Inertial Measurement Unit MPU6050

The IMU MPU6050 is widely used in the robotics industry and hence Arduino provides libraries for calibration and global data extraction. These libraries were used to find the linear and angular displacement of the quadcopter.

Summary

In this chapter the various parts of the experimental setup were finalised based on the various constraints of accuracy, time for manufacture, cost etc.. The setup selected to be built was a 2D equivalent of the 3 DOF planar model discussed in the previous chapter.

The size of the Quadcoptor and Gun was decided such that the effect of thr recoil was significant but not unmanageable.

The mathematical model of the full setup was made and validated by simulating its behaviour on MATLAB. The behaviour matched closely with the behaviour recorded by the Inertial Measurement Unit(IMU) mounted on the actual setup. The control gains found in the previous chapter were applied onto this model and the behaviour was found to be close to "Critically Damped".

Chapter 5

Experiments

5.1 Benchmarking of Gun Aim and Precision



Figure 5.1: Benchmarking affixed to the ground 1



Figure 5.2: Benchmarking affixed to the ground 2

The objective of this experiment was two fold:

1. To create a sight for the gun that would become the true aim of the gun – establishing the reference point for future accuracy measurements.
2. To quantify the precision of the gun – the angular spread and the pattern of the spread for the air gun.

Methodology-

1. The gun was affixed rigidly to a heavy platform that would not move due to the recoil of the gun.
2. A target was placed 1760 mm from the muzzle of the gun. 10 rounds were fired and the maximum distance between the bullet holes was measured. This was continued until the distance stopped increasing.
3. Using the distance between the muzzle and the target, and the spread diameter of the bullets the angular precision of the gun was calculated.
4. A laser was affixed below the gun which aimed at the center of the spread pattern of the bullets. This is the true aim of the gun for further accuracy experiments.

Observations

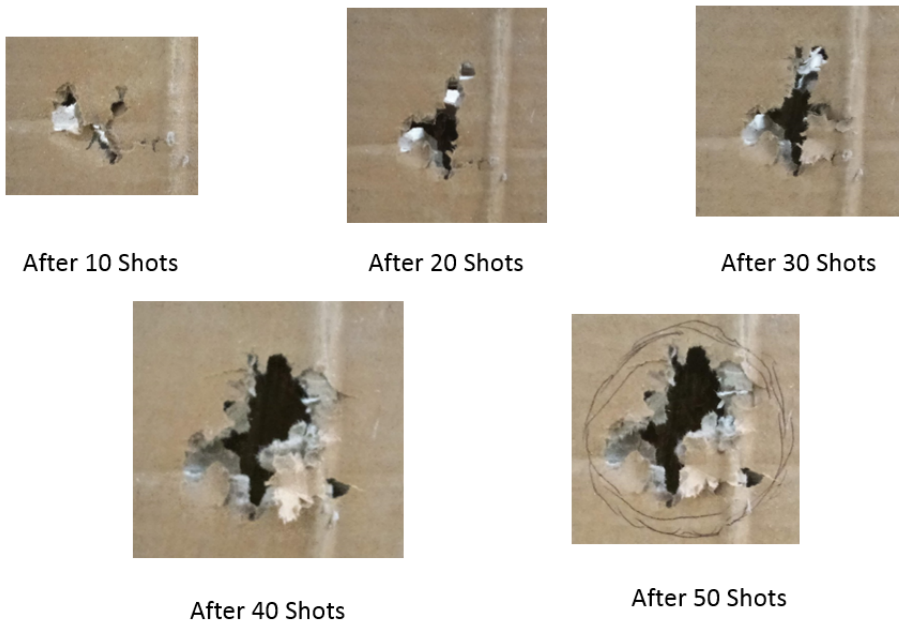


Figure 5.3: Progressive Shot Patterns

Result

1. The angular precision of the gun is 1.5 degrees
2. A laser was set up to benchmark the true aim of the gun

5.1.1 Benchmarking of the Gun Aim and Precision on Setup

The Objectives of this experiment were to quantify the accuracy and the precision of the gun when mounted on the setup. That is, when it was not rigidly attached to the ground.

There are 2 possible reasons for the parameters in question(Accuracy, Precision, etc.) to vary from the previous benchmarking results, and they are

1. The setup is adding to the instability
2. The motors on the Quadcoptor are adding to the instability

In order to check both aspects, the main experiment was split into two parts, one where the Quadcopter motors are off and another when the motors rotate at their rated speeds.

The rest of the methodology of this experiment was the same as that for the previous Benchmarking Experiment.

The Observations are

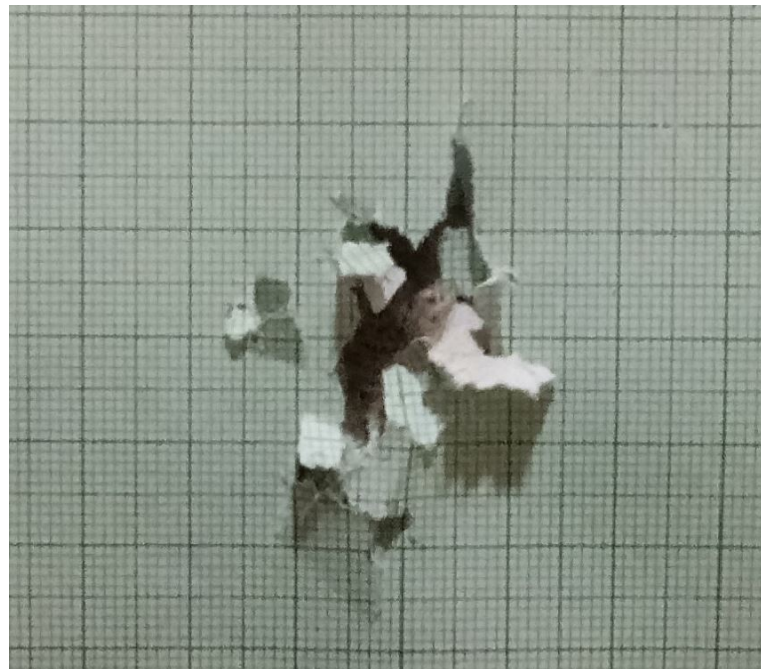


Figure 5.4: Scatter pattern of gun mounted on setup

Results

The precision of the gun is unaffected and stays at 1.5 degrees

The Accuracy of the gun is affected and the gun shoots 0.5 degrees lower than its intended target

5.1.2 Effect of control Algorithms on Precision, Accuracy and Firing Rates

Objectives

1. 1. To find the effect of various control strategies and control gains on the Precision, Accuracy and Firing Rates of the Gun mounted Quadcoptor
2. 2. To tune the control gains of the most desirable control strategy to achieve optimal precision, accuracy and firing rate

Methodology

1. Implement a basic PD controller onto the Quadcoptor.
2. Measure the precision, accuracy and settling time of the setup.
3. Change the values of control gains to optimize the precision, accuracy and settling time
4. Change control strategy(to PID and including the linear displacement) and go to step 2
5. Choose the most optimal control strategy and control gains for the same

Observations

Parameters of Experiment										
Experiment No.	Type of Experiment	KP for θ state	KD for θ state	KI for θ state	KP for x state	KD for x state	KI for x state	Precision in degrees	Accuracy offset in Degrees	Settling Time in seconds
1	PD controller for θ state	10	0.1	NA	NA	NA	NA	8.5	0.5	1.7
2	PD controller for θ state	100	0.05	NA	NA	NA	NA	8	0.5	1.8
3	PID controller for θ state	100	0.05	0.005	NA	NA	NA	5.166	1.03	1.8
4	PID controller for θ state	100	0.5	0.05	NA	NA	NA	3.044	0	1.9
5	PID controller for θ and x state	100	0.5	0.05	50	NA	NA	3.348	0	0.5
6	PID controller for θ and x state	100	0.5	0.05	50	0.5	NA	3.025	0	0.41

Figure 5.5: Experiments with different controllers)

5.2 Results and Discussion

The experiments were carried out till a maximum balance of accuracy, precision and Settling time was achieved. the following table lists the performance of each control logic and its gains.

Parameters of Experiment										
Experiment No.	Type of Experiment	KP for θ state	KD for θ state	KI for θ state	KP for x state	KD for x state	KI for x state	Precision in degrees	Accuracy offset in Degrees	Settling Time in Seconds
1	Benchmarking Ground	NA	NA	NA	NA	NA	NA	1.5	NA	NA
2	Benchmarking Setup	NA	NA	NA	NA	NA	NA	1.5	0.5	2
3	PD controller for θ state	10	0.1	NA	NA	NA	NA	8.5	0.5	1.7
4	PD controller for θ state	100	0.05	NA	NA	NA	NA	8	0.5	1.8
5	PID controller for θ state	100	0.05	0.005	NA	NA	NA	5.166	1.03	1.8
6	PID controller for θ state	100	0.5	0.05	NA	NA	NA	3.044	0	1.9
7	PID controller for θ and x state	100	0.5	0.05	50	NA	NA	3.348	0	0.5
8	PID controller for θ and x state	100	0.5	0.05	50	0.5	NA	3.025	0	0.41

Figure 5.6: Experiments with different controllers

This table shows the various controllers and the control gains used vs parameters of concern such as accuracy, precision and settling time. We can conclude from this table that of the controllers tested on the setup, the PID controller applied onto both x and θ states reduces the settling time and increases the precision and accuracy the most.

This was the expected outcome as most commercial Quadcoptors use a variation of the same controller. The added benefit of these experiments is the correlation between the various controllers and their effects on accuracy, precision and settling time. This information may allow better performance of Quadcopter UCAV's with commercial controllers by, for example compensating the reduction in accuracy by aiming upwards by a certain amount.

Chapter 6

Conclusions

The methodology used in this report can be used to increase the accuracy, precision and firing rate of Multi-rotor UCAV's. The control strategies explored, while very rudimentary show that having prior knowledge of the dynamics of the Multi-rotor and the gun recoil can significantly improve the behaviour of the Multi-rotor UCAV's.

The Angular states majorly affect the accuracy and precision of the Quadcoptor while the Linear states significantly affect the settling time thereby having an impact on the firing rate.

The models developed in the course of this report show that the performance of a Multi-rotor UCAV is strongly correlated to only a subset of the states involved in the full model. This approach can be used to simplify the tuning of the UCAV and save on computational time. The method of "analogous spring-mass-damper" is very effective in obtaining a "critically damped" behaviour of the UCAV's, which in turn optimised the accuracy, precision and settling time. This method also makes it easier to tune control gains in an otherwise very complex Non-Linear system.

In the future, a more conclusive experimental setup can be built which can take into account more of the complex effects of rotational drag forces, blade flapping and bulk wind velocity. Further inclusion of these effects in the simplified model will also allow for higher fidelity simulations which will reduce the time required for finding control gains. Having more sensors like multiple IMU's and cameras with sensor fusion techniques will

allow for better estimation of states leading to better overall control. Having a real gun or an equivalent mechanism that can reproduce the effects of a real gun will make the experiments more realistic and take into picture the effect of various actuating mechanisms used in real guns.

References

- [1] “A successful french helicopter,” 1924. Flight 24 January p47.
- [2] “An mq-9 reaper unmanned aerial vehicle flies a combat mission over southern afghanistan.,” 2008. U.S. Air Force Photo / Lt. Col. Leslie Pratt [Public domain].
- [3] “Tikad drone by duke robotics,” 2018.
- [4] L. Brits, “Euler angles wikipedia the free encyclopedia,” 2004.
- [5] A. Gibiansky, “Quadcopter dynamics and simulation,” 2012.
- [6] “Ashani mark -ii pistol,” 2009.
- [7] “A diy gun mounted on a quadcoptor.”
- [8] W. R. Young, “The helicopters. the epic of flight,” 1982. Chicago: Time-Life Books. p. 28.
- [9] “Drone warfare: The death of precision,” 2017. Bulletin of the Atomic Scientists.
- [10] C. Kennedy and J. I. Rogers, “Virtuous drones?,” *The International Journal of Human Rights*, vol. 19, no. 2, pp. 211–227, 2015.
- [11] “The simulation of the human-machine partnership in ucav operation,” 2013. College of Aeronautics, Northwestern Polytechnical University, Xi'an 710072, China.
- [12] A. Dowd, “Drone wars: risks and warnings,” 2014. College of Aeronautics, Northwestern Polytechnical University, Xi'an 710072, China.

[13] “Euler angles wikipedia the free encyclopedia,” 2004.

[14] “Euler’s equations (rigid body dynamics).”